

University of Liège
Faculty of Applied Sciences
Aerospace and Mechanical Engineering Department

Thermal issues settlement and test procedure investigation of OUFTI-1 nanosatellite

Thesis submitted
in partial fulfilment of the requirements
for the degree of
Master in Aerospace Engineering

by

Jean-Philippe NOËL

Advisor: Prof. Pierre Rochus

June 2010

Contents

1	Introduction	1
1.1	The OUFTI-1 Thermal Control Subsystem	2
1.2	Outline of the dissertation	3
2	Integration of batteries (part 1)	5
2.1	Problem statement	6
2.2	The thermal control system	11
2.2.1	Heaters as source of energy	11
2.2.2	The decision to reheat	12
2.2.3	How to arrange thermostats	17
2.2.4	The unregulated supply	20
2.3	The mechanical support	22
2.3.1	Qualitative proposition and resulting realization	22
2.3.2	Dynamic behaviour	27
2.3.3	Wasting of energy and insulation means	28
2.3.4	System integration	28
2.4	Conclusions	31
3	Integration of batteries (part 2)	33
3.1	Thermal modelling	34
3.1.1	The Geometric Mathematical Model (GMM)	35
3.1.2	The Thermal Mathematical Model (TMM)	40
3.2	Test procedure	44
3.2.1	Test objectives	44
3.2.2	Test setting up	46
3.2.3	Test procedure	55
3.3	Conclusions	62
4	Minor issues	63
4.1	The dissipation transistor in hot case	64
4.2	The COM amplifier in hot case	66
5	Conclusions	68

<i>CONTENTS</i>	ii
Appendix 1	71
Appendix 2	82

List of Figures

2.1	Predicted temperature within the batteries, according to [1]	7
2.2	Fixing system of the BATtery Printed Circuit Board (BAT PCB) onto the Electrical Power Subsystem Printed Circuit Board (EPS PCB) as foreseen in [1]	8
2.3	Deformation state exhibited under vacuum by KOKAM battery (<i>KOKAM SLB 603870H</i>) : the battery twists (top Figure) and crinkles (bottom Figure)	9
2.4	Snap-action bimetal actuator of a mechanical thermostat	14
2.5	The 4BT-2 thermostat	16
2.6	Characteristics of the selected 4BT-2 thermostats	17
2.7	An example of redundancy scheme	17
2.8	A ideal quad-redundant wiring scheme	18
2.9	The parallel arrangement	19
2.10	The series arrangement	19
2.11	The battery support as previously designed	22
2.12	The reviewed battery support from a qualitative point of view (exploded view)	25
2.13	The reviewed battery support from a qualitative point of view (integrated view)	25
2.14	The reviewed battery support from a quantitative point of view (exploded view)	26
2.15	The reviewed battery support from a quantitative point of view (exploded view)	26
2.16	Integration of the battery thermal control system and mechanical support	29
2.17	The battery subsystem in OUFTI-1	30
3.1	Displayed points of view of the battery system	35
3.2	First plan of the battery system (support): plan view	36
3.3	Second and third plans of the battery system (support): side view (top Figure) and front view (bottom Figure)	36
3.4	Conformity of the ESARAD geometric model, seen from CATIA	37
3.5	Conformity of the ESARAD geometric model, seen from ESARAD	37

3.6	Conformity of the ESARAD geometric model, seen from CATIA (2)	38
3.7	Conformity of the ESARAD geometric model, seen from ESARAD (2)	38
3.8	The whole battery system, as drawn in ESARAD: the support and one battery	39
3.9	The whole battery system, as drawn in ESARAD: the support and both batteries	39
3.10	The whole battery system, as drawn in ESARAD: the support, both batteries and the cover	40
3.11	Thermal modelling results, given as an example	41
3.12	Thermal modelling results, given as an example (2)	42
3.13	Thermal modelling results, given as an example (3)	42
3.14	Testing set-up outline	46
3.15	The copper temperature-controlled panel (rear side) and the brazed heating coil	47
3.16	Time constant τ estimation of the battery cooling process	49
3.17	Relationship between the battery time constant τ and the importance of the thermal conductance between the battery support and the temperature-controlled panel	50
3.18	Copper temperature-controlled panel on insulating Teflon feet	51
3.19	Insulating MLI blanket covering up the whole set-up	51
3.20	Thermocouples positioning and numbering (graphical display)	52
3.21	Test electrical set-up	54
3.22	Test simulation as seen from the batteries thermostats-side	58
3.23	Test simulation as seen from the support and the cover	59
5.1	Display of the support and the cover eigenmodes	71
5.2	The battery support: First eigenmode – 733 Hz	72
5.3	The battery support: Second eigenmode – 1219 Hz	73
5.4	The battery support: Third eigenmode – 1434 Hz	74
5.5	The battery support: Fourth eigenmode – 1787 Hz	75
5.6	The battery support: Fifth eigenmode – 2102 Hz	76
5.7	The cover: First eigenmode – 1460 Hz	77
5.8	The cover: Second eigenmode – 2826 Hz	78
5.9	The cover: Third eigenmode – 3254 Hz	79
5.10	The cover: Fourth eigenmode – 3773 Hz	80
5.11	The cover: Fifth eigenmode – 5493 Hz	81

Acknowledgments

I am deeply grateful to all the people who contributed, somehow or other, to the carrying out of this dissertation.

First, I would like to express my gratitude to Professor Pierre Rochus who gave me the opportunity to get involved in the rewarding OUFTI-1 project. In particular, I acknowledge him for his relevant and enlightened advices.

I would like to thank Professor Michel Hogge, Dean of the Applied Sciences Faculty, and Professors Jean-Claude Golinval and Gaëtan Kerschen for serving on my jury panel. I also acknowledge Didier Granville who accepted to take part in this jury, as exterior member.

Among the members of the OUFTI-1 team, who I appreciated to work with, my special thanks go to Amandine Denis and Jérôme Wertz who constantly oversaw and guided my work year-round.

Finally, I am indebted to Tanguy Thibert and Lionel Jacques, from the *Centre Spatial de Liège*, for their endless and valuable technical support.

I particularly thank Tanguy Thibert for his careful reading of the third chapter of this dissertation and Lionel Jacques for his equally meticulous reading of the second chapter.

Chapter 1

Introduction: OUFTI-1, a battery-equipped CubeSat

The CubeSat concept originates from the proposition of Prof. Twiggs of Stanford University. According to him, it was proposed “*as a vehicle to support hands-on university-level space education and opportunities for low-cost space access.*”

At its most fundamental level, a CubeSat is a 1 kg $100 \times 100 \times 100$ millimetres cube-shaped spacecraft. Its definition is scalable and CubeSat units may subtend larger systems. Actually, up to 6 unit CubeSats are proposed.

The standardisation of the interface between the launch vehicle and the CubeSat is the central element of the concept. It allows group launch and so reduced costs along with increasingly frequent opportunities.

Numerous universities and organisations have fallen in behind Prof. Twiggs, and more than sixty missions are developed nowadays.

In 2006, the University of Liège decided to take the plunge at the instigation of Luc Halbach. His proposition to put into orbit the D-STAR amateur-radio digital-communication protocol as primary payload of a CubeSat begins the project.

The main purpose of OUFTI-1, as it was named for Orbital Utility For Telecommunication Innovation, is thus to keep remote communications going, either for housekeeping or experimental purposes. The second goal of OUFTI-1, considered as its secondary payload, is the formal on-orbit qualification of a digitally-controlled electrical power supply.

The OUFTI-1 mission consequently demands electrical power in great

measure, either to communicate with a ground-station on Earth or to supply its electronic components.

The Sun provides this required power during sunshine periods. However, to keep the spacecraft alive during eclipse periods, it seems unavoidable to store a part of the solar power in batteries. This introduction of batteries within OUFTI-1 involves numerous issues tackled in this work.

1.1 The OUFTI-1 Thermal Control Subsystem

Chris J. Savage, from the European Space Research and Technology Centre, introduces the role of the thermal control of a spacecraft like this [2]:

“Spacecraft thermal control — that is the control of spacecraft equipment and structural temperatures — is required for two main reasons: (1) electronic and mechanical equipment usually operate efficiently and reliably only within relatively narrow temperature ranges [...].”

“Heat is generated both within the spacecraft and by the environment. Components producing heat include [...] electronic devices and batteries. [...] Heat from the space environment is largely the result of solar radiation. Heat is lost from the spacecraft by radiation, mainly to deep space. The balance between heat gained and heat lost will determine the spacecraft temperatures.”

The first thermal study of OUFTI-1 was carried out by Stefania Galli, during the academic year 2007-2008, in her feasibility study of the CubeSat. The necessity to guarantee each of the on board hardware components a proper thermal environment was thereto underlined. The electronic components as well as the batteries were cited as critical components according to their thermal requirements. A fully passive thermal control was then envisaged, carefully selecting the optical properties of the spacecraft to reach an admissible operating temperature range.

In 2008-2009, Lionel Jacques succeeded her and was the first to concentrate his whole work on the thermal control of OUFTI-1. His work focused on a detailed study of the spacecraft thermal behaviour. He developed increasingly complex, and therefore relevant, thermal modellings of the CubeSat using the European Space Agency softwares.

The knowledge gained through these numerical studies enables him to precisely identify three thermal issues, not resolved thanks to passive control so far, namely:

- the too cold temperature of the batteries in cold case.
- the detrimental heat generation of an electrical transistor.
- the equally detrimental heat generation of a communication amplifier.

L. Jacques suggested solutions to settle these issues. According to him, the first of them inevitably leads to the use of an active thermal control system that he designed. In addition, the enhancement of conductive thermal paths would resolve the second and the third issues.

Nevertheless, his solutions were neither studied in details (for instance, the heaters control loop was still at an early stage) nor concretised.

Thus, the purposes of my work were clearly established at the beginning of the year. Each of those three issues had to be definitely settled and the relevancy of their solutions had to be proved thanks to a thermal test programme to be defined, and conducted if possible. The title chosen for this thesis naturally results from those objectives.

Nevertheless, in the course of the year, the battery issue in cold case turns out to be more complex than it first seemed to be, involving thermal, mechanical and electrical aspects. These aspects were separately considered up to then, leading to some inconsistencies in the design process.

Conscious of the importance of the battery integration in OUFTI-1, my work was then reoriented and exclusively focused on the battery issue settlement.

1.2 Outline of the dissertation

The study of the battery problem is the heart of this thesis. For the sake of clarity, it is split into two chapters, the second and the third chapters of this dissertation.

Chapter 2 provides qualitative information about the design of the battery system. It begins with a comprehensive statement of the battery issue. This statement may be the major ideational progress proposed in this work. It enables a better understanding of the underlying requirements and constraints and almost naturally leads to a consistent design of the battery system.

The second and third parts of this chapter address the design of the battery system, first of all from a thermal point of view and then from a

mechanical point of view.

In the second part, a complete active thermal control system is built in the purpose of preventing the battery temperature from dropping below a prescribed threshold. This control system compromises:

- heaters as active source of energy,
- a reheating decision-making mechanism, actually mechanical thermostats,
- an approach of redundancy,
- considerations about energy wasting.

The third part discusses the mechanical design of the battery system. It considers the battery under-vacuum deformations and the shortness of the CubeSat to propose a review of the existing support.

Chapter 3 aims at complementing the previous chapter thanks to quantitative information.

The thermal behaviour of the battery system is thereto analysed thanks to ESATAN-TMS software in a first part. The numerical model is shortly described and is followed by some examples of information made accessible through the modelling.

The knowledge gained at this stage leads to the second part of the third chapter, the definition and the simulation of a test procedure, in the purpose of confirming the proper performance of the battery system.

Chapter 4 approaches, before concluding this dissertation, the two minor thermal problems highlighted last year, namely the electrical transistor and the communication amplifier. Relying on the work carried out by L. Jacques, the chapter briefly reviews the technical state of those problems along with their envisaged solutions.

Chapter 2

Integration of batteries: problem statement, thermal control system and mechanical support

This chapter introduces the study of the OUFTI-1 battery system. It mainly contains qualitative information about its design, successively addressed from both thermal and mechanical aspects.

Based on the work carried out last year by L. Jacques [1], a complete active thermal control system is thereto developed. The active energy source is first addressed followed by the research and the development of a reheating decision-making mechanism. The questions of the system redundancy and of its electrical supply are then discussed in order to conclude the first part of this chapter.

Mechanical aspects of the problem are secondly considered. A deep review of the battery support is introduced to fulfil the inherent OUFTI-1 constraints and to settle critical issues left aside so far, the battery under-vacuum deformations essentially. Eventually, the integration of the thermal control system earlier mentioned within the new battery support is described.

To make the reading of this chapter easier and to free the reader from an in-depth knowledge of L. Jacques's work, the OUFTI-1 battery issue is first stated prior to beginning any technical consideration.

2.1 Problem statement

Batteries and CubeSats have never got along so well and issues resulting from their association do often occur. Indeed, a battery is a fragile component, relatively heavy and bulky. Just the opposite, a CubeSat is a light and confined satellite which is not capable, in essence, of protecting a battery against the unfriendly space environment.

Many CubeSats stand as examples of this inconsistency. The CubeSat *Delfi-C³*, from the University of Delft in the Netherlands, is a battery-less satellite, while it carries other complex and fragile systems such as scientific payloads, wireless sun sensors or deployable solar panels. The choice not to use batteries is justified like this [3] : *Delfi-C³ does not carry a battery system. Batteries are notorious sources of trouble in nano-satellites and have even caused missions to fail.*

Other examples can be quoted. The AAU-CubeSat team members (from the University of Aalborg, Denmark) noticed that the satellite's batteries lost their capacity after a month in vacuum. In their opinion, this issue could be resolved by pressing the batteries between aluminium plates to prevent them from expanding.

Thermal testing results of the CUTE-1 CubeSat (from the University of Tokyo, Japan) showed that a monitoring of some components temperature was essential, especially the batteries temperature.

At last and without being thorough, the AeroCube-2 (from the Aerospace Corporation, USA), CAPE-1 (from the University of Louisiana, USA) and SSETI Express (from many European universities and supported by ESA) CubeSats faced problems related to batteries malfunction.

Nevertheless, OUFTI-1 will take two batteries on board because of the electricity supply they provide during eclipse periods. Thereby, the challenge to be taken up is to overcome practical issues raised by their presence. Three main problems can be enumerated.

The thermal issue

The first issue, and definitely the most delicate, is to ensure that all the batteries' thermal requirements are fulfilled. Indeed, the required artificial thermal environment to be established is far from being an on-orbit one.

From a thermal point of view, the battery issue is well summarised in the following extract of L. Jacques's work's conclusion [1] :

“In the cold case, simulations showed that the batteries would undergo too low temperatures and that they were out of their temperature ranges when coming out of eclipse. A heating system has therefore been designed [...]”

Actually, when coming out of eclipse, the batteries begin their charging phase. According to their specifications (see datasheet in Appendix 2), this phase involves a minimum admissible temperature of 0°C . Unfortunately, a temperature of about -15°C is foreseen by the numerical simulations, as depicted below (dotted line) [1].

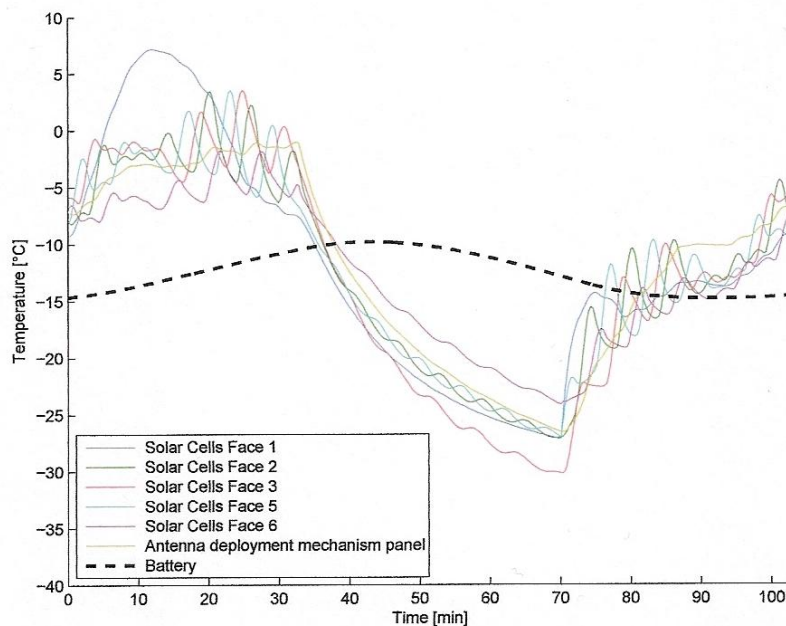


Figure 2.1: Predicted temperature within the batteries, according to [1]

Consequently, the use of an active control system, actually heaters, seems unavoidable. However, the control of this active system, its required power, its activation threshold and the reduction of its losses (that is to say the increase of its efficiency) are four new questions issuing from the design of such a system.

Several control solutions were dismissed last year, in favour of an independent electronic control loop entirely dedicated to the heater system, for the sake of simplicity and reliability.

In addition, the option of one heater per battery coupled with three temperature sensors seemed to be the most convenient. Again, this choice

improved the redundancy and the reliability of the control system.

This being so, numerical simulations [1] concluded that two 250 mW heaters, actuated when a threshold of 5°C is transgressed, are sufficient to maintain, in the worst case, the battery temperature within an acceptable range. Both values (250 mW and 5°C) are such that, even if one heater fails, temperature of the two batteries does not drop below 0°C .

In order to improve the efficiency of the heaters, the BAT PCB has to be insulated at best, radiatively just as conductively.

Covering the batteries with an aluminium tape was showed to be the easiest way of insulating them radiatively. Moreover, this solution was efficient and appeared to be essential to reach the desired level of temperature.

Conductive losses have to be stopped as well. L. Jacques foresaw the solution of combining Titanium components and Nylon or PTFE washers to ensure structural resistance, stiffness as well as poor heat conductivity of the fixing system. This idea is illustrated in Figure 2.2.

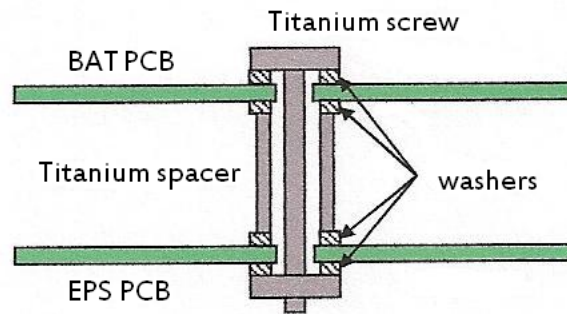


Figure 2.2: Fixing system of the BATtery Printed Circuit Board (BAT PCB) onto the Electrical Power Subsystem Printed Circuit Board (EPS PCB) as foreseen in [1]

Mechanical issues

The second issue to be pointed out, and maybe the most unpredictable, is the tangible deformation state experienced by batteries under vacuum. Indeed, a large majority of off-the-shelf batteries suitable for taking place within a CubeSat exhibits this unwanted behaviour.

The battery model chosen to take place in OUFTI-1 — KOKAM SLB 603870H battery (see Appendix 2) — clearly undergoes these deformations.

The Figure 2.3 displays such a battery, twisted and crinkled, after a stay in a vacuum vessel at the *Centre Spatial de Liège* (CSL) (pictures taken from [4]).



Figure 2.3: Deformation state exhibited under vacuum by KOKAM battery (*KOKAM SLB 603870H*) : the battery twists (top Figure) and crinkles (bottom Figure)

That deformation state along with the inconveniences it involves lead to consider the need to pack the batteries to prevent them from expanding and consequently preserve their functionalities.

Structural considerations and excessive dimensions of the batteries are responsible for a third and last issue. In fact, the thickness of the batteries combined with an inadequate support can lead to detrimental vibration amplitudes. Inside OUFTI-1, the batteries are located between the EPS PCB and the experimental Electrical Power Subsystem Printed Circuit Board (xEPS PCB). The interval size is small and welcomes, however, some EPS PCB and xEPS PCB's components, the BAT PCB as well as both batteries. This shortness drastically reduces the allowable vibration magnitude

of the batteries and their support to prevent shocks with electronic components. In fact, the clearance between a battery and the closest EPS PCB's component is shorter than a millimetre.

In addition, the unavoidable battery casing introduced above was not considered and makes almost unsolvable this problem of available space management.

At the beginning of the academic year 2009-2010, different elements related to integration of batteries within OUFTI-1 were established and not questioned anymore, namely:

- the need to actively control their temperature during cold phases of the satellite's orbit using, from a threshold of $5^{\circ}C$, 250 mW heaters.
- this last need being periodic, the associated control system has to include a control loop regularly estimating the need to reheat.
- the under-vacuum deformations have to be managed, that is tolerated, reduced or merely cancelled out.

Just the opposite, the unanswered or partially answered questions related to that integration were:

- how to control the reheating phases of the batteries, that is how to electrically supply the heaters when needed, for given heater power and activation threshold, and to switch them off when a sufficient temperature level is reached ?
- how to manage the under-vacuum deformations exhibited by batteries ?
- how to manage the available interval between the EPS PCB and the xEPS PCB where the batteries have to take space, considering the need to pack them according to the last question ?
- assuming an accommodation of the battery support design to meet the answers of both previous questions, is a thermal control system update needed ? In particular, the insulation means described above depend on the batteries' environment and would clearly be prone to such an update.

Those elements will be, one after the other, studied and then resolved in this work to reach a complete and consistent design of the support and the thermal control system of the batteries. At this stage, this system will be ready to be tested, hopefully validated and ultimately integrated within OUFTI-1.

2.2 The thermal control system

The unavoidable necessity to actively bring batteries heat during OUFTI-1's orbit cold phases is definitely the most important and valuable conclusion underlined last year by the Thermal Control Subsystem (TCS).

Its role did not stop at this only identification, though. The different lines followed to resolve the battery problem were outlined in the previous section. They deal with the questions of the active energy source, of its unwanted wasting and of the reheating decision-making process. The answers brought are the use of heaters, of radiative and conductive insulators and of an electronic control loop, respectively. High-level details were considered above while low-level details are to be found in [1].

However, those lines of solution do not make the battery problem completely resolved because of several constraints not considered so far. For instance, the reliability, the mass and the manufacturing capability of an electronic control system, the available space management mentioned above or the battery under-vacuum deformations are such constraints.

This section dedicated to the battery thermal control system intends to develop a consistent design meeting each requirement and each constraint of such a system.

The section is divided into four parts, each of them answering a clearly stated subproblem with its own constraints: the choice of an active energy source is discussed in the first one, the reheating decision-making mechanism is studied in the second and third parts while the electrical power supply discussion lies in the last part.

A fifth part belongs to the battery system settlement topic, that is the prevention of the battery-heater system from energy wasting. However, because of its dependence on the battery mechanical support design, it will be addressed later, in Section 2.3.4.

2.2.1 Heaters as source of energy

The simple choice introduced last year to use heaters as active source of energy is definitely relevant. Thus, I do neither discuss this choice again nor question it.

Gilmore [5] introduces heaters in this way: “*Heaters are [...] sometimes required in a thermal design to protect components under cold-case environ-*

mental conditions [...] Heaters may also be used with thermostats [...] to provide precise temperature control of a particular component.”

The most common and widely used type of heater, in space applications, is the patch heater, made up “*of an electrical-resistance element sandwiched between two sheets of flexible electrically insulating material [...]*” [5]. Regularly, they are fitted with an adhesive side to be glued wherever needed.

This being so, numerical simulations [1] concluded that two 250 mW heaters are sufficient to maintain, in the worst case, the batteries’ temperature within an acceptable range, that is to say above 0°C. This result will be confirmed further when simulating the validation test procedure (in Figure 3.22 within the Section 3.2.3.).

Moreover, as developed below, the heaters are electrically supplied by the batteries themselves. If one assumes a minimal 2.5 V supply, the heaters’ resistance are merely equal to

$$R = \frac{V^2}{P} = 25 \Omega$$

A patch heater has a second main property, as well as its resistance, namely its geometry (shape and dimensions). To maximise the heat transfer to the battery, the heater’s and the battery’s geometries have to be matched at best.

The OUFTI-1’s selected batteries are *KOKAM SLB 603870H* lithium batteries (see datasheet in Appendix 2). They are rectangular box-shaped with dimensions of 69.5 × 37.5 × 6.5 millimetres. For the sake of redundancy and sufficient capacity, two batteries will be taken on board.

Considering this configuration and the numerical results, the choice made last year and confirmed here goes for two *MINCO HK5377R26.3L12* NASA approved-heaters (see datasheet in Appendix 2), one per battery. They are made up of a 26.3 Ω resistance element wrapped up in an insulating Kapton envelope and are 59.4 × 35.6 millimetres-sized.

2.2.2 The decision to reheat

“*Almost all heaters allow some sort of control over their operation.*” [5]

Usually, such a control system demands

- a ground-commandable relay to enable or disable the control capability.

- a short-circuit protection, actually a fuse.
- according to circumstances, a mechanical or electronic switch to turn the power supply on and off.

Basically, heaters can be controlled through two different ways. If their activation is needed only during special events (before hydrazine thrusters firing, for instance) or if they are left on all the time, the control is simply ground-commanded.

Conversely, if an automatic control is needed, in this case to keep a component above a given temperature level, a thermostat or a solid-state controller, that is a reheating decision-making device, is besides involved. Sophisticated spacecraft even have the capacity to tailor the temperatures at which heaters are turned on to environmental conditions, thanks to their onboard computers.

Considering the OUFTI-1's heaters, the end sought is to keep a component (actually the batteries) above a given temperature level, and then required a decision-making device.

Mechanical thermostat

According to Gilmore [5], mechanical thermostats are the most common way of controlling heaters used to periodically reheat components and for which consumption is to be minimised. Usually, those thermostats “*consist of small, hermetically sealed cans containing a switch driven by a snap-action bimetal actuator*”.

The schematic view in Figure 2.4 exemplifies this mechanism.

The electrical contact is switched on between a movable and a stationary metallic parts depending on the deformation of a bimetallic disc. The properties of this bimetal (composition and dimensions) determine the temperature at which the contact is effective.

A mechanical thermostat is characterized by its *set point*, the temperature at which it turns on, and its *dead band*, the difference between the set point and the temperature it switches off.

Gilmore [5] recommends not to choose dead band lower than 4°C , to prevent the thermostat from fast cycling on and off.

An important consideration to be mastered when making use of mechanical thermostats is the knowledge of their failure modes.

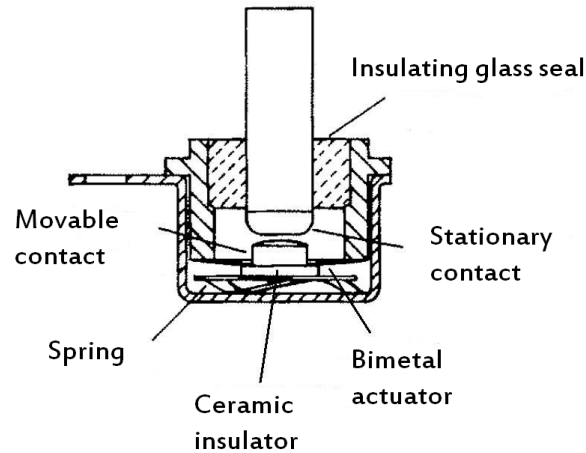


Figure 2.4: Snap-action bimetal actuator of a mechanical thermostat

Thus, beyond its proven reliability, such a thermostat can sometimes

- fail closed, i.e. the heater being supplied, causing a continuous and detrimental energy consumption.
- fail open, i.e. the heater not being supplied, causing the loss of the component to be reheated without excessive power consumption.
- dither, causing the set point to drift lower and then the loss of the component.

Gilmore [5] reviews the primary causes of these failures in this way : “*The primary causes of failure are internal contamination, manufacturing defects, excessive narrowness of the dead band, inadequate screening, improper installation, excessive current, and pitted contacts*”.

Consequently, our choice has to be made considering the following elements:

- no dead band lower than 4°C , at the risk of dithering.
- if possible, no set point below 0°C , at the risk of forming ice (a thermostat can contain ambient air and water) on the contacts and then failing open.
- no high current because of possible closed failure resulting from welding of the contacts.

- no contaminant (e.g. outgassed material) within the thermostat environment, at the risk of preventing contacts from closing or leading to dithering as a result of an increase in electrical resistance between contacts and an internal heating.

Nevertheless, before considering elements such as the set point, the dead band or the failure modes of a thermostat in the decision making process, constraints in terms of mass and dimensions have to be fulfilled.

For instance, Gilmore [5] acquaints Elmwood mechanical thermostats as common thermal control device. However, the lightest space-qualified Elmwood thermostat weights no less than 8,5 grams. If one assumes the necessity of two thermostats per battery, the total mass budget accounts for 34 grams, that is to say twenty percents of the total allocated mass budget for the battery system (including the batteries themselves, their mechanical support, etc.). Clearly, this mass is unacceptable. In addition, dimension considerations also lead to the rejection of such thermostats.

The Klixon 4BT-2 thermostat

The solution is brought by *Klixon Precision Thermostats*. Indeed, within the *Tiny Stat Miniature Thermostat* series, whose datasheet is given in Appendix 2, lies the *4BT - 2* model which perfectly fits our drastic constraints. The three drawings in Figure 2.5 illustrate that device.

Its properties are listed below:

- a mass of approximately 0,2 gram.
- sizes not exceeding a centimetre in each of the three dimensions.
- capability to undergo space environment (NASA qualified).
- wide range of operating temperature, from $-15^{\circ}C$ to $175^{\circ}C$.
- unique differential of $16.7^{\circ}C$
- tolerance over the operating temperature and the differential of $4.4^{\circ}C$

The last choice which has still to be made is the selection of an operating temperature, the differential being imposed.

It should be emphasized that, following the manufacturer's definition, the mechanical thermostats considered here are said to be *normally closed*, that is they open on temperature rise and re-close as the controlled device

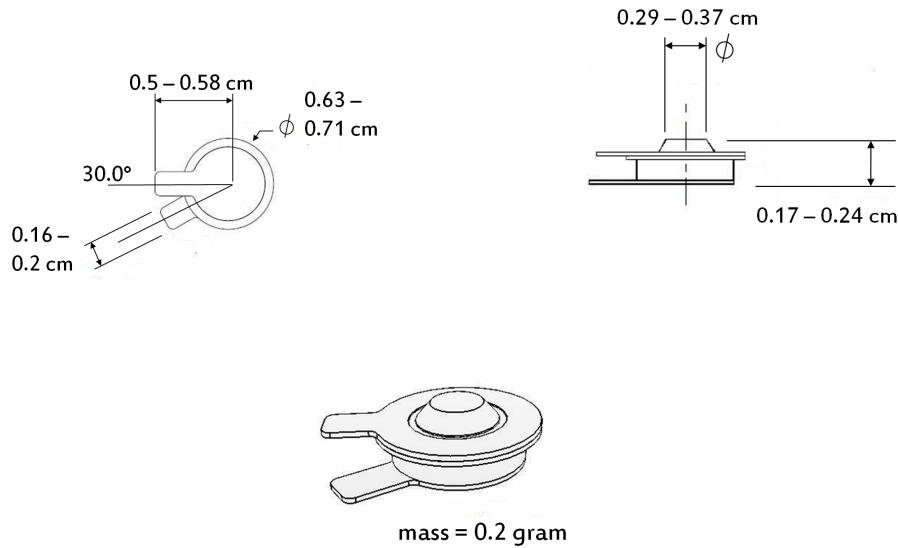


Figure 2.5: The 4BT-2 thermostat

cools at a predetermined temperature.

Moreover, their operating temperature is defined as being the temperature at which they open, thus contradicting the definition given above.

This being so, following the need to supply the heaters prior to undergoing negative temperatures, the chosen operating temperature is 23.9°C . Thus, considering the differential and its tolerance, the thermostat will close, at worst, at 2.8°C .

The Figure 2.6 summarizes the characteristics of the OUFTI-1 mechanical thermostats (*Klixon* 4BT-2):

- the operating temperature, the temperature at which a normally closed thermostats opens, according to *Klixon*: 23.9°C .
- the set point, the temperature at which a thermostat turns on, according to Gilmore [5]: 7.2°C .
- the differential, defined from the operating temperature (*Klixon*): 16.7°C .
- the dead band, defined from the set point (Gilmore): 16.7°C .
- the uncertainty intervals: $\pm 4^{\circ}\text{C}$.

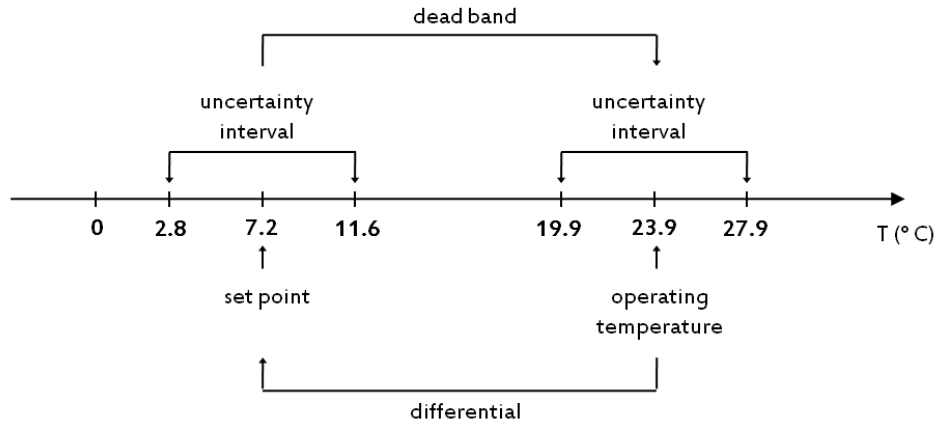


Figure 2.6: Characteristics of the selected 4BT-2 thermostats

2.2.3 How to arrange thermostats

The desired level of redundancy determines the required number of thermostats along with their arrangement, i.e. the way of (electrically) connecting them.

For example, a redundancy scheme is presented in Figure 2.7.

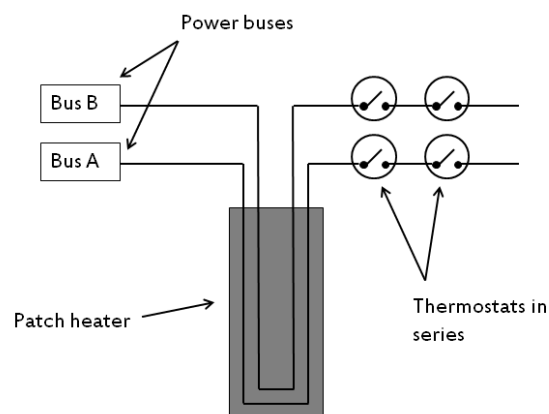


Figure 2.7: An example of redundancy scheme

On this example, the heater consists of two resistance elements in a single-patch envelope and is then redundant itself. Those two resistances

are supplied by separate power buses. Series-redundant thermostats provide a *single-fault tolerance* in the event that closed failure would occur.

Nevertheless, single-fault redundancy is not fully realized so far. Indeed, the circuit is dead if a thermostat fails open.

In OUFTI-1, the power bus is not duplicated and the employing of split resistances within a unique patch-envelope is therefore meaningless.

However, considering a simply-supplied heater, different wiring schemes can be envisaged to lay out thermostats depending on the level of reliability to be ensured.

The most reliable of them is presented in Figure 2.8. The scheme contains two branches in parallel, each of them being composed of two series-thermostats. Essentially because of cost considerations (this scheme involves the need of eight thermostats for the whole system), this solution was rejected in spite of its capability to be prepared for single open and closed failures. Indeed, two successive failures are required to disable the thermostatic control.

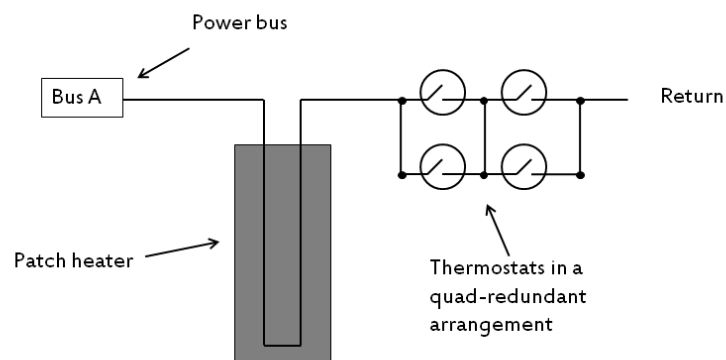


Figure 2.8: A ideal quad-redundant wiring scheme

Those cost considerations lead us to focus on a configuration based on only four thermostats, two per battery.

Different arrangements, which can be actually found in satellites, involve two thermostats, and consequently a reduced cost along with a loss of reliability compared with the quad-redundant arrangement. The simple series

and parallel arrangements are successively depicted in Figure 2.9 and 2.10.

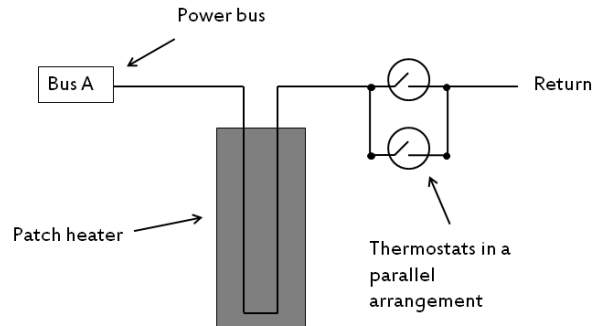


Figure 2.9: The parallel arrangement

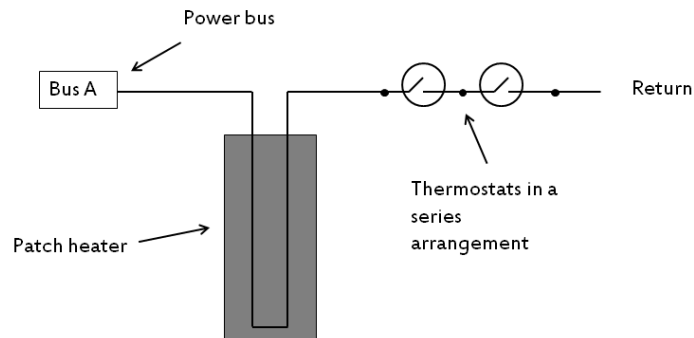


Figure 2.10: The series arrangement

The former is capable of confronting an open failure but involves an unlimited power consumption in the case of a closed failure. Thus, this possible continuous flow of energy from the satellite budget to the heaters and the risk to lose the battery because of an excessive level of temperature are clearly detrimental.

The latter is, of course, able to cope with a closed failure while an open failure involves only the battery freeze without compromising the mission through an uninterrupted power consumption.

The two-thermostats series arrangement was thus selected among others possibilities as being the best compromise, considering cost, reliability and redundancy, mass and dimensions considerations.

The decision matrix given below summarizes the decision-making process outlined in this section.

	Single-fault redundancy	If open single failure, mission not jeopardized?	If closed single failure, mission not jeopardized?	Size	Mass	Cost	Decision
Quad-arrangement	✓	—	—	✗	✗	✗	✗
Parallel double-arrangement	✗	—	✗	✓	✓	✓	✗
Series double-arrangement	✗	✓	—	✓	✓	✓	✓

Table 2.1: Decision matrix related to the thermostats arrangement decision-making process

2.2.4 The unregulated supply

When considering the need of heaters within a spacecraft, the main parameter to be defined is their electrical resistances. Indeed, this choice leads to a given dissipated power, intended to reheat a predetermined component.

The univocal correspondence between a resistance and a dissipated power assumes the supply voltage constancy. However, the choice made last year is to supply the thermostat-heater system directly with the output battery voltage, and then without resorting to a bus regulated voltage.

This choice is not question and implies an unstable supply voltage depending on the battery charge state. This almost unpredictable data justifies (as detailed in [1]) the 2.5 V supply assumed when designing the heaters, whereas the battery cut-off voltage is equal to 2.7 V.

This particular supply, directly coming from the batteries to be reheated themselves, raises the following question: how to reheat an empty battery?

In fact, the batteries' capacity was chosen to ensure a very limited depth of discharge, and then to considerably extend their expected life. The gap

thus existing between their cut-off voltage and their minimal voltage in activity will be utilised to supply the heaters, with a consequent little loss of expected life.

2.3 The mechanical support

Even if the design, the manufacture and the validation (this latter being discussed in the section 3.2) of the battery support are no part of the TCS's duties, I nevertheless dedicate a section to this issue because of my involvement within the design process and because of its direct relationship with the battery thermal control system.

This section first describes the qualitative design review I proposed and the consequent concrete design reached by STRU subsystem. This review is introduced considering the problems involved by the existing support at the beginning of this year.

Some mechanical details come next in readiness for the validation procedure establishment, outlined in Section 3.2.3.

The third and fourth sections address the insulation means completing the battery thermal control system and the final integration of every hardware component introduced in this chapter.

2.3.1 Qualitative proposition and resulting realization

The mechanical support considered at the end of the academic year 2008-2009 is depicted in Figure 2.11.

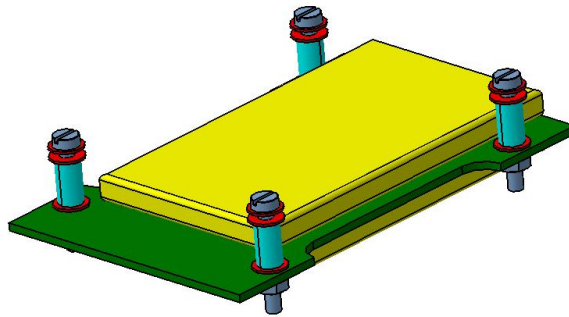


Figure 2.11: The battery support as previously designed

Its main and interesting characteristics are:

- the batteries positioning, one upon the other.
- its material, a glass fibre-reinforced polymer (FR4) typically used as Printed Circuit Board.

- its fixing system (also displayed in Figure 2.2), combining insulating polymer washers (in red) and titanium screws.
- its shape, a rectangle.
- considering a heater glued on the main side of a battery, the intersection between the reheating thermal path and the second battery.

The unresolved problems linked to this design are now listed:

- the deformation state exhibited by batteries under vacuum clearly noticed during a test process at the CSL. These unpredictable deformations were well known, even though not clearly understood, but no concrete solution was envisaged except for the possibility of packing them in an aluminium casing.
- that casing not being more than a suggestion, the question of the available space was not addressed anymore. However, the conjugation of the batteries arrangement (one on top of the other, see Figure 2.11), the need of a casing wrapping the batteries and the height of the EPS PCB's and xEPS PCB's components imposes an unsolvable space problem.
- the mechanical integrity of the existing support, although studied and enhanced thanks to titanium screws, was weakened by its particular fixing system compared with the PCBs one.

It appeared that the settlement of those issues cannot be reached thanks to a simple adjustment of the existing support. Therefore, I proposed to deeply review this support following the next guidelines:

1. to better exploit the available space within the satellite, arranging the batteries next to each other. This element complies with the confined and limited available space between the EPS PCB and the xEPS PCB.
2. to perform the integration of the support thanks to the Pumpkin structure's endless screws rather than fixing it to the contiguous PCBs, improving its mechanical behaviour.
3. to consider *a priori* the battery under-vacuum deformations in the design process of the support.

This naturally leads to the new support design drawn in Figures 2.12 and 2.13, as proposed at the end of January 2010. The Figure 2.12 stands for an exploded view of the integrated system displayed in Figure 2.13.

These illustrations are said to be qualitative because they only reflect the conceptual guidelines stated above. Thus, even if proportions and orders of magnitude are respected, no geometric information is strictly correct and is even not to be considered.

The responses to the three foregoing guidelines are:

1. the effective arrangement, side by side, of the batteries.
2. the corner holes to welcome the CubeSat structure's screws.
3. in the purpose of cancelling out the under-vacuum deformations, the design of reinforcers, surrounding the rectangular-shaped batteries, and of a cover to be screwed upon the support.

The transition from the Figures 2.12 and 2.13 to a concrete realization was completely carried out by STRU subsystem. The result is given in Figures 2.14 and 2.15. The detailed process history is to be found in [6].

The qualitative support and its quantitative equivalent are given on two successive pages to make the comparison easier and to clearly underline their conceptual similarity.

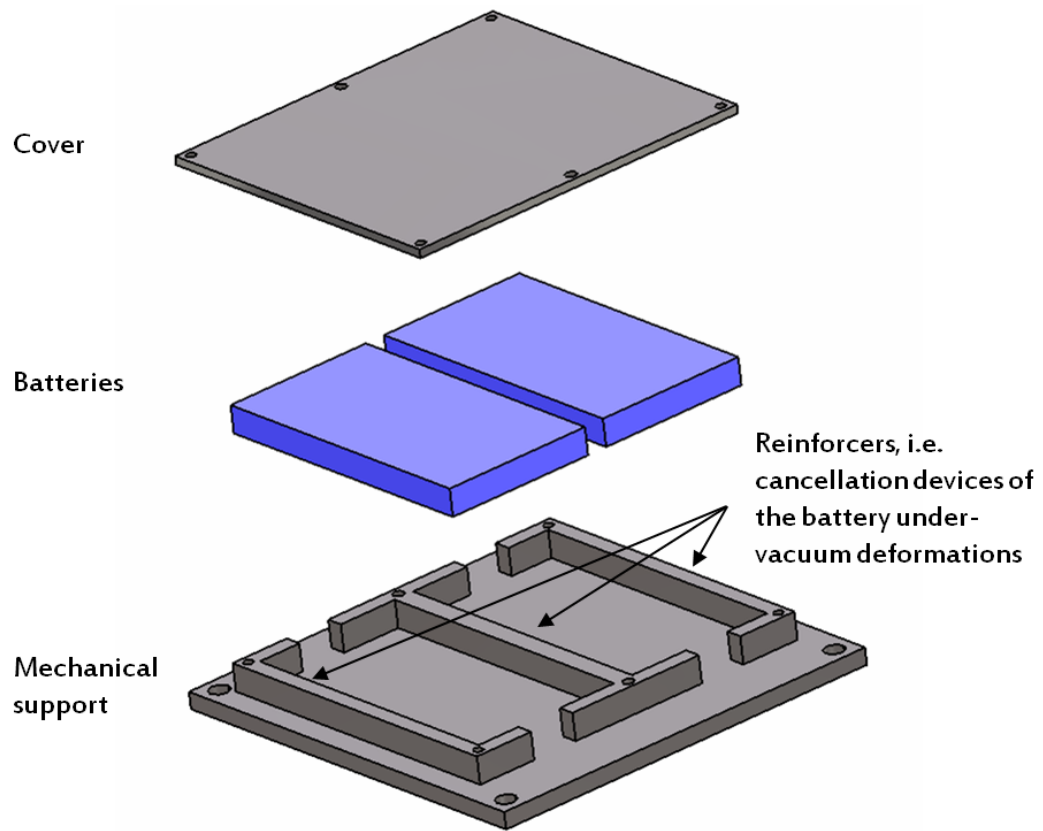


Figure 2.12: The reviewed battery support from a qualitative point of view (exploded view)

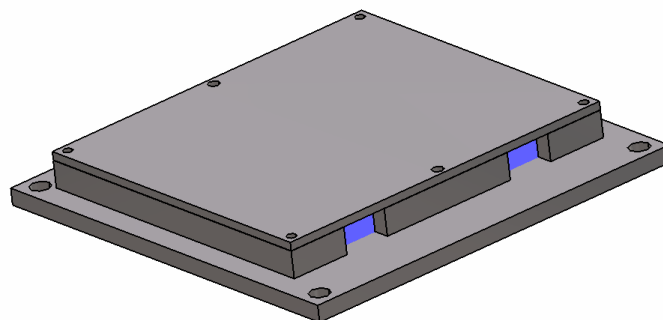


Figure 2.13: The reviewed battery support from a qualitative point of view (integrated view)

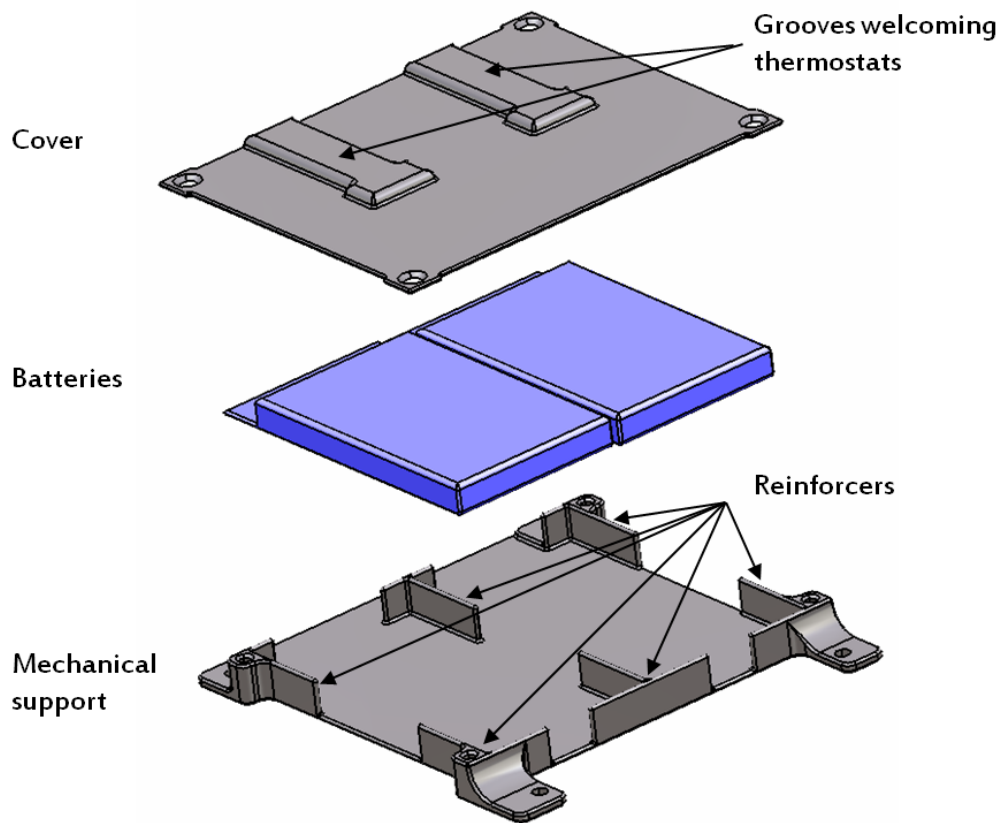


Figure 2.14: The reviewed battery support from a quantitative point of view (exploded view)

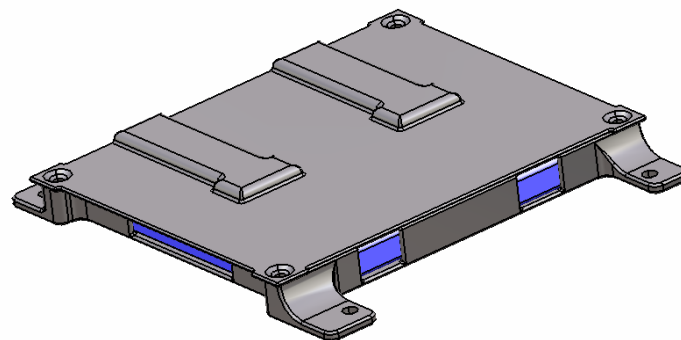


Figure 2.15: The reviewed battery support from a quantitative point of view (exploded view)

2.3.2 Dynamic behaviour

The aim of this subsection is not an in-depth study of the battery system dynamic behaviour. Thus, for instance, its natural frequencies, mode shapes or response under a given solicitation are not addressed.

However, to prepare the validation test procedure outlined in Section 3.2.3., the modal features — the natural frequencies actually — of the support and its cover, independently considered from the whole system, are of interest. This interest will be justified when addressing the detection of possible cracks due to battery under-vacuum deformations.

Thereby, in order to build a comprehensive and coherent validation procedure, those features are proposed here.

The finite element computation was performed assuming, as boundary condition, the support and the cover clamped through their four corner holes.

The first five natural frequencies of the support are listed in Table 2.2.

Support	Natural frequencies [Hz]
First Mode	733
Second Mode	1219
Third Mode	1434
Fourth Mode	1787
Fifth Mode	2102

Table 2.2: The first five natural frequencies of the support

As for the cover, its five first natural frequencies are listed in Table 2.3

Cover	Natural frequencies [Hz]
First Mode	1460
Second Mode	2826
Third Mode	3254
Fourth Mode	3773
Fifth Mode	5493

Table 2.3: The first five natural frequencies of the cover

The corresponding mode shapes of both structures, rather than being displayed here and then overloading the content of this chapter, are gathered in Appendix 1, because of their reduced interest.

2.3.3 Wasting of energy and insulation means

The support redesign performed, the batteries' thermal environment is now completely defined. Thus, the energy wasting from the heater-battery system to this environment can be studied in the purpose of being minimised thanks to well-considered insulation means.

Following simplicity, reliability and cost considerations, aluminium was chosen to manufacture the support and its cover introduced above. This choice incidentally leads to an efficient radiative insulation. Indeed, thanks to its low infra-red emissivity ($\epsilon = 0.05$), an aluminium surface, whether it also experiences conductive heat transfer, behaves like an excellent insulator in radiation [7].

However, aluminium high thermal conductivity is likely to involve important and detrimental conductive losses. To overcome this issue, the decision was made to insert a Polyester netting (see datasheet in Appendix 2) layer between the batteries and the support on one hand, and between the batteries and the cover on the other hand.

This netting, no thicker than a half millimetre, is typically used, in space applications, in the purpose of preventing conductive heat transfers.

2.3.4 System integration

The last section of this chapter intends to describe the assembly of all the hardware components introduced above, namely:

- the two batteries,
- the two heaters,
- the four thermostats,
- the Polyester insulator,
- the support,
- the cover.

The Figure 2.16 helps to image their arrangement.

The first step in integrating this system is to glue the four thermostats on the batteries upper sides, two per battery. The exact location is the centre of the batteries and has to comply with the cover grooves positioning.

The Stycast 2850FT Epoxy resin (see datasheet in Appendix 2) will be used with a catalyst 24LV. This choice follows high thermal conductivity and low outgassing property (TML = 0.38% \leq 1% requirement, CVCM = 0.01% \leq 0.1% requirement) considerations. The resin must dry during a 24 hour-period at room temperature whereas the catalyst needs an additional 4 hour-period drying at 60°C.

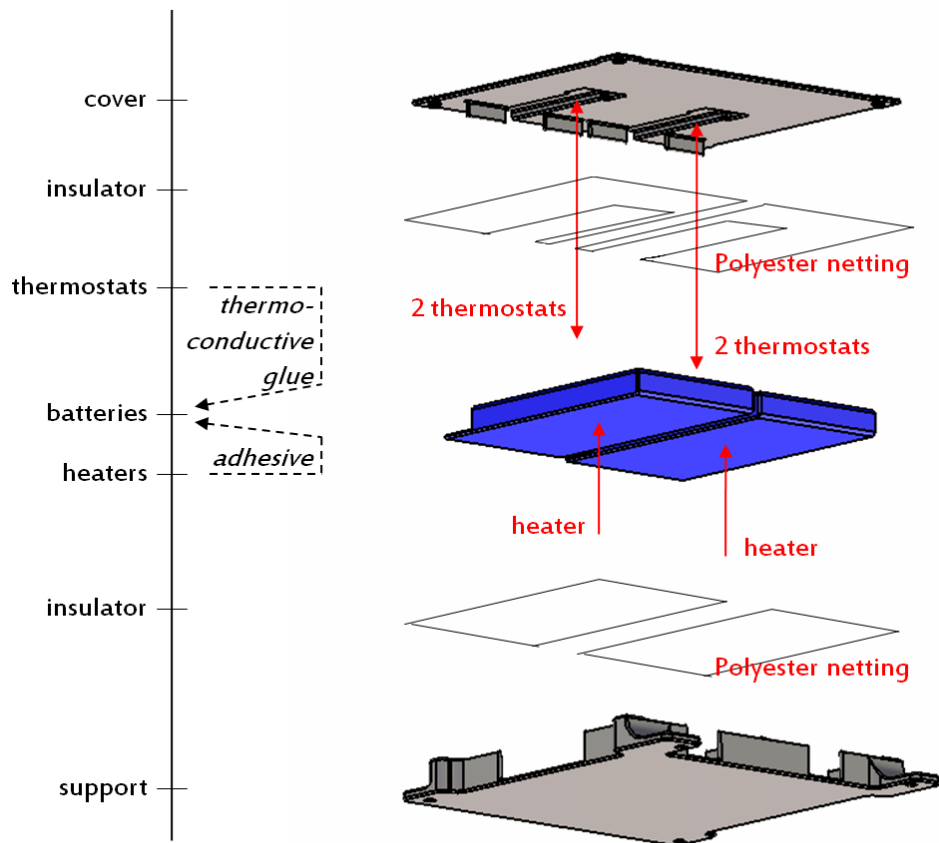


Figure 2.16: Integration of the battery thermal control system and mechanical support

Secondly, thanks to their pressure sensitive adhesive sides, the heaters are bonded on the batteries lower sides.

The last stage consists in successively overlaying upon the support:

- two Polyester netting layers, fitting the batteries' dimensions, posi-

tioned side by side,

- the two batteries along with their heaters (2) and thermostats (4),
- two Polyester netting layers, surrounding the cover's grooves, positioned side by side,
- the cover.

Lastly, by the way of illustration, the Figure 2.17 shows the whole battery subsystem integrated within OUFTI-1.

It is positioned between the EPS PCB and xEPS PCB, closer to the latter because of the former's components height. Comprehensive information about its exact location and about the available space management is to be found in [6].

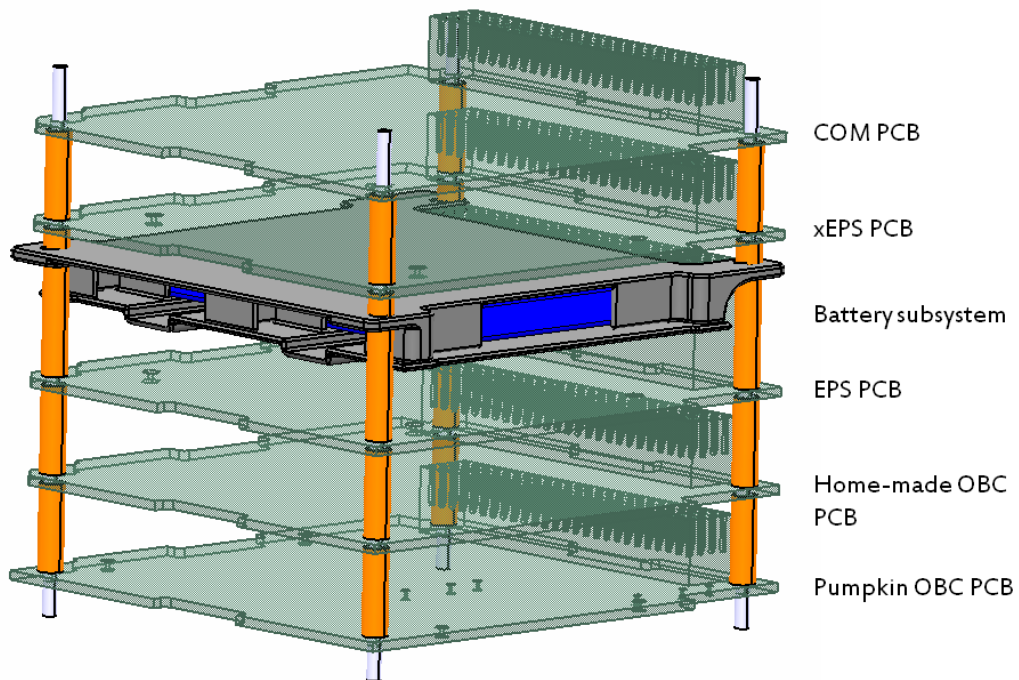


Figure 2.17: The battery subsystem in OUFTI-1

2.4 Conclusions

This chapter intended to build a consistent design of the battery subsystem in OUFTI-1.

This cannot be achieved without a comprehensive statement of the problems to be overcome. Indeed, rather than tackling the battery issue from different points of view according to different subsystems, the method followed here considers, from the beginning, each issue no matter its origin — thermal, mechanical, etc. — as an input constraint.

The handling of the battery problem under its global nature and the identification of the need to resolve it from a high-level approach are definitely the key elements introduced and developed here.

This being so, the problem statement naturally led us to each of the hardware components introduced throughout the chapter.

Different design components were simply confirmed or adjusted compared with the work carried out last year [1], for instance the heaters or the battery supply.

Other elements were completely reviewed, considering constraints not underlined or gathered so far, to reach, such as the thermal control system using thermostats or the battery mechanical support.

However, many questions remain unanswered, for example:

- is the heaters' power sufficient to prevent the batteries' temperature from dropping below $0^{\circ}C$, considering the mechanical support redesign?
- what are the effect and the relevancy of the insulation means in terms of energy wasting?
- in worst hot case, do the insulation means imply temperature level lower than the allowable upper limit?
- what are the consequences of a heater loss?
- what is the influence of the batteries' output voltage instability?
- how long last a reheating phase, considering the thermostats' operating temperature and the heaters' dissipated power?
- what is the electrical consumption involved during such a phase?
- what does imply the batteries' inertia in terms of heat spread?

- etc.

These questions emphasize the need of numerical information, obtained through computational and/or experimental ways. The following chapter will fill this gap, first addressing a numerical modelling of the battery subsystem in the ESATAN-TMS environment prior to establishing its validation test procedure.

Chapter 3

Integration of batteries: thermal modelling and test procedure

This third chapter continues the study of the battery system largely initiated in the previous chapter. It combines the qualitative information discussed so far in the context of a design process with complementary quantitative information.

The numerical as well as the experimental ways are followed to better understand the system thermal behaviour, through a numerical modelling in a first part followed by a test investigation in a second one.

The development of a detailed thermal modelling of the battery system is thus first addressed. This first part of the chapter intends to be brief. Indeed, the central purposes to be achieved are first the definition of a thermal validation test and then its numerical simulation. In this context, the thermal modelling appears to be an additional tool to reach a comprehensive study of the battery system, rather than an end in itself.

The battery system validation test is finally discussed. The thermal, mechanical and electrical test objectives are first stated. After performing the description of the set-up of a thermal test, this latter is defined and simulated. Accounting for the numerical results, a review of the test objectives is finally conducted.

3.1 Thermal modelling

The solvers used in this section are ESARAD (European Space Agency Radiative analysis) and ESATAN (ESA Thermal ANalysis) softwares, presently assembled in a unique environment known as *ESATAN - Thermal Modelling Suite*. As anticipated, this section does not give details about these softwares or the numerous steps involved in the development of a thermal model. L. Jacques [1] provides an in-depth description of those elements.

Nevertheless, to understand the outline of an analysis developed in ESATAN-TMS along with its layout, a short description of the underlying mathematical model is not dispensable.

To be as clear and complete as possible, here is what is said in the ESATAN-TMS User Manual:

The type of mathematical model which is used for the analysis is the so-called lumped parameter model. This is formulated by dividing the geometric model into a number of pieces. Each of these pieces is then represented as a point, with the physical properties of the piece lumped onto the point. Connections are then established between pairs of points to represent conductive and radiative couplings with other parts of the model.

This set of points and connections may be viewed as a network, with the points as nodes. The term node is, in general parlance, also used to describe the piece of the geometric model which is represented by the actual node of the network.

The behaviour of this network can be described by a set of coupled differential equations whose coefficients are the lumped values of the nodes. Among the values which are lumped are: heat capacity, [...], conductances to adjacent nodes, radiative exchanges to nodes, temperature.

Lumping of the temperature has an important consequence: the material of the node is treated as being isothermal. This has implications for the radiation calculations. [...]

As the distinction between ESARAD and ESATAN underlines so, the different steps of analysis mentioned in this quote are split up into two major models: the Geometric Mathematical Model and the Thermal Mathematical Model.

3.1.1 The Geometric Mathematical Model (GMM)

The GMM, developed and processed in ESARAD, first contains the geometrical information of the problem, created thanks to simple geometric primitives (from the rectangle to the paraboloid) and logical operations.

Secondly, the geometry nodal breakdown is carried out in the GMM, that is the creation of the isothermal nodes network based on the continuous and physical geometry. This being so, the computation of the nodes radiative couplings can be performed. The information proposed in this section is displayed on the following figures.

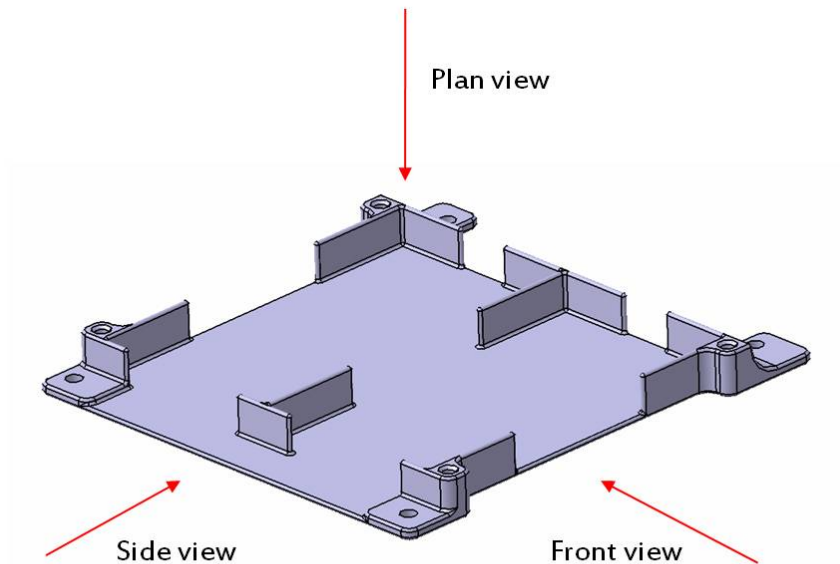


Figure 3.1: Displayed points of view of the battery system

The plans used to build the geometry of the problem are depicted in Figures 3.2 and 3.3. Their three points of view are clarified in Figure 3.1.

In addition, the conformity between the physical geometry of the battery system and its model in ESARAD is established in Figures 3.4, 3.5, 3.6 and 3.7.

Lastly, the whole battery system, as drawn in ESARAD, is displayed in Figures 3.8, 3.9 and 3.10.

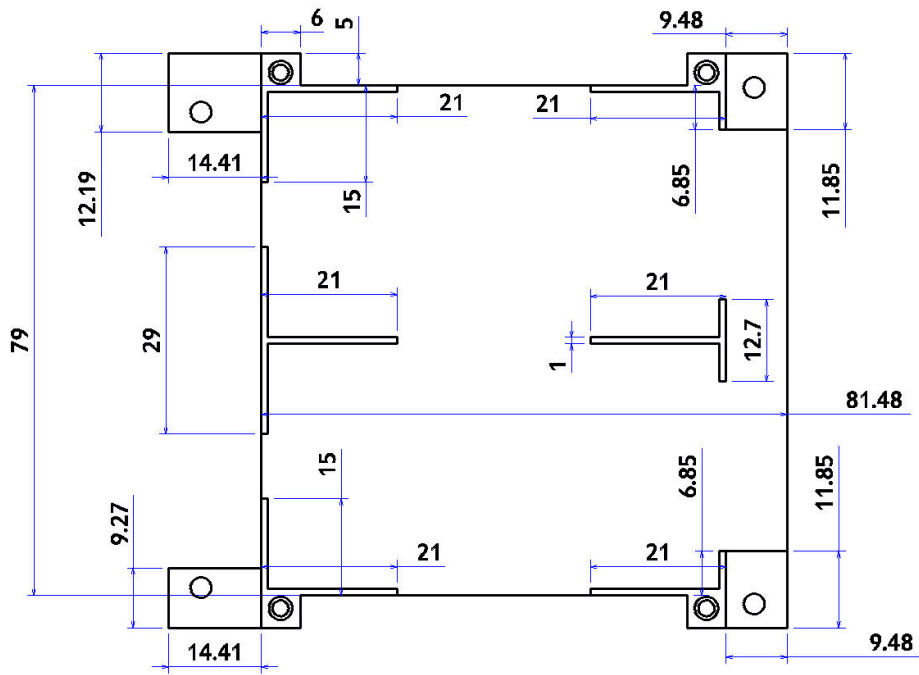


Figure 3.2: First plan of the battery system (support): plan view

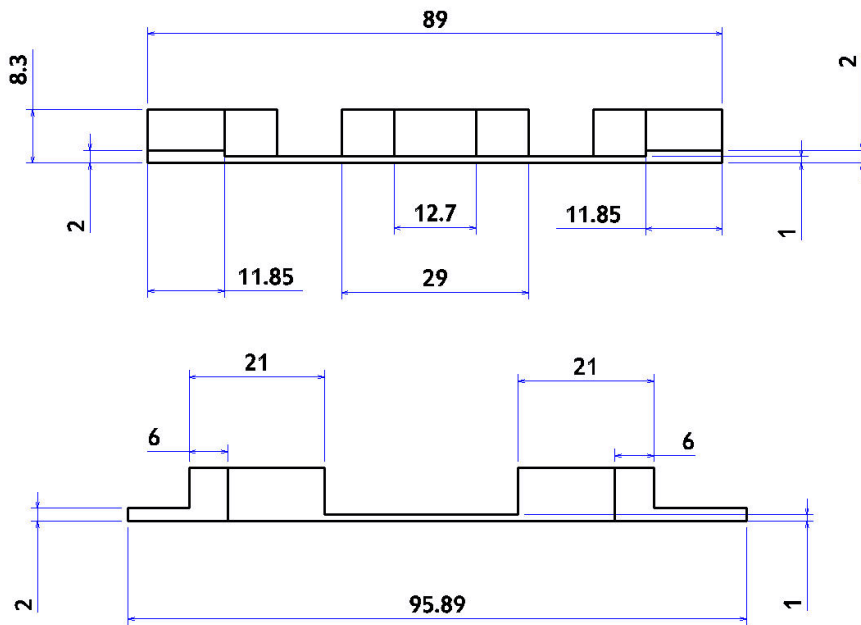


Figure 3.3: Second and third plans of the battery system (support): side view (top Figure) and front view (bottom Figure)

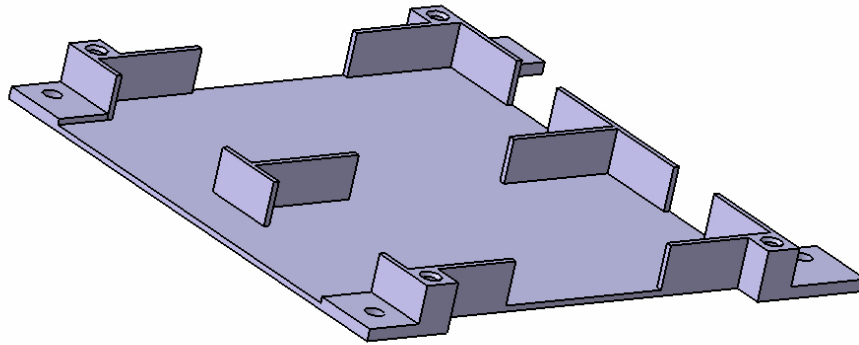


Figure 3.4: Conformity of the ESARAD geometric model, seen from CATIA

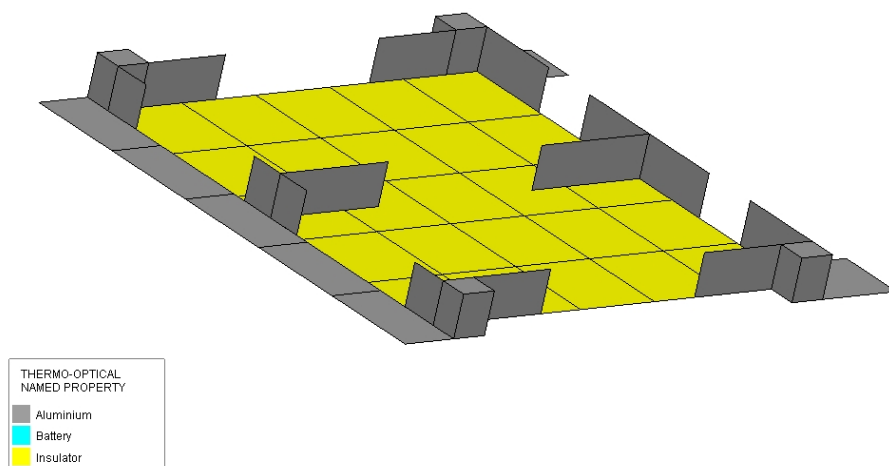


Figure 3.5: Conformity of the ESARAD geometric model, seen from ESARAD

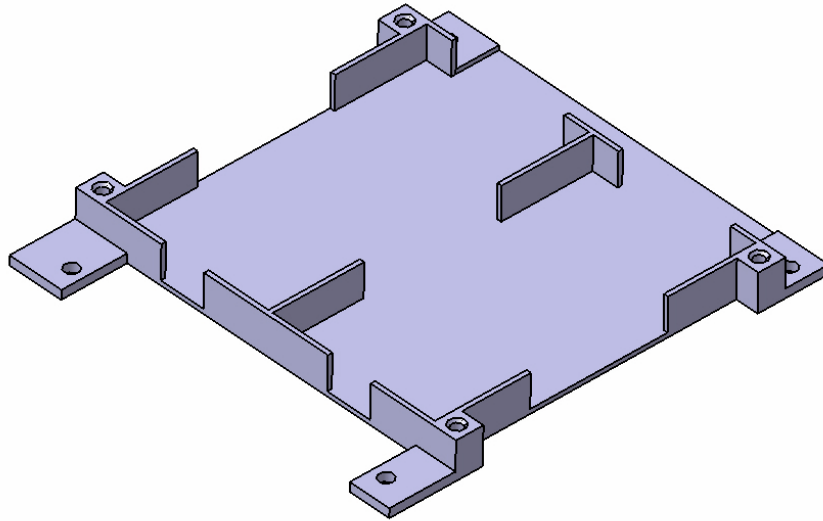


Figure 3.6: Conformity of the ESARAD geometric model, seen from CATIA (2)

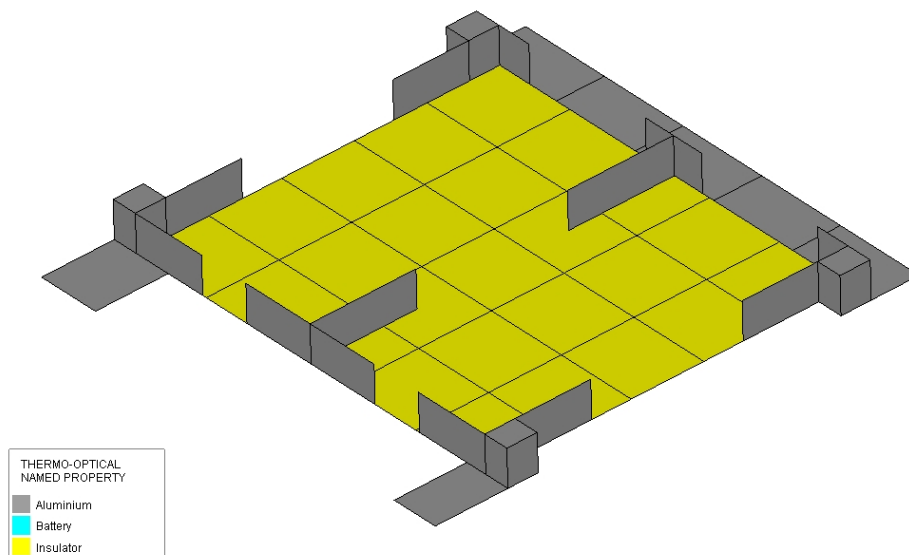


Figure 3.7: Conformity of the ESARAD geometric model, seen from ESARAD (2)

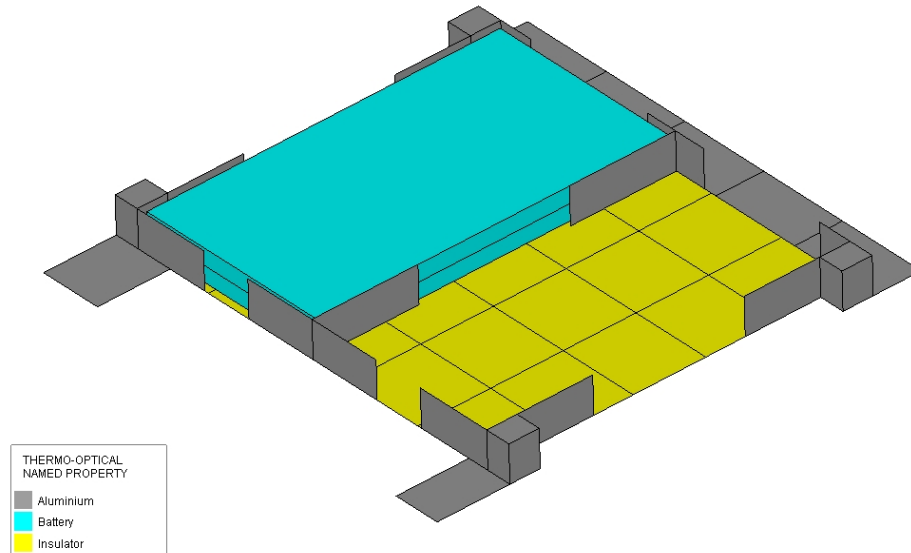


Figure 3.8: The whole battery system, as drawn in ESARAD: the support and one battery

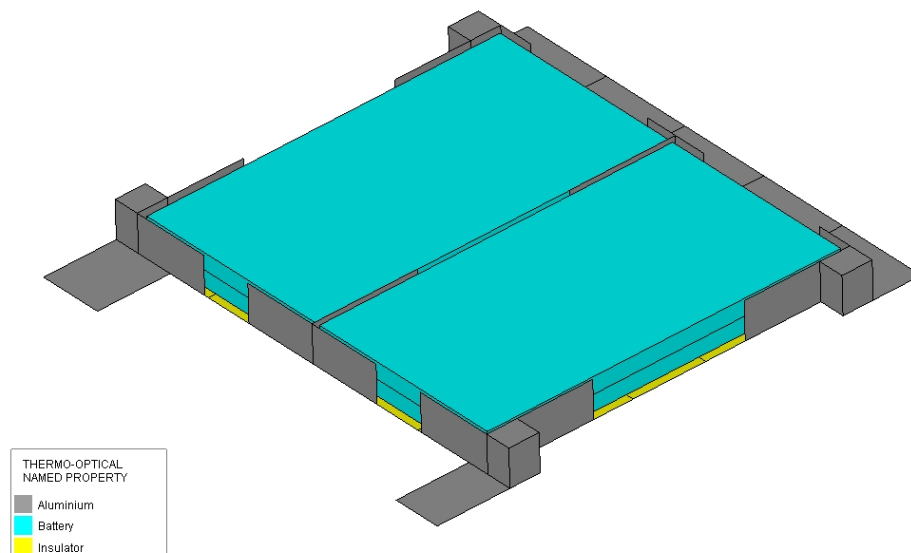


Figure 3.9: The whole battery system, as drawn in ESARAD: the support and both batteries

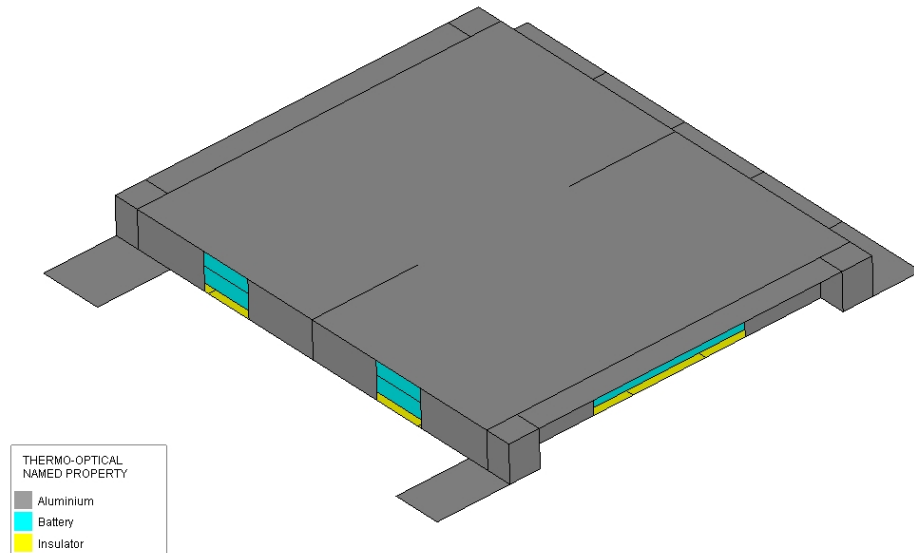


Figure 3.10: The whole battery system, as drawn in ESARAD: the support, both batteries and the cover

3.1.2 The Thermal Mathematical Model (TMM)

At this stage, the nodes network and the radiative couplings between those nodes are known. To complete the data set involves in the writing of the coupled differential equations to be solved, heat capacities, heat dissipation/inputs/losses and conductive links have to be computed and listed.

This being done, the discrete temperature field is to be computed as the solution a coupled system of heat balances.

For practical purposes, the hand-computed heat capacities, heat inputs and conductive links are given to *Matlab* where the ESATAN appropriate files are built, providing flexibility, sensitivity analysis capability, etc.

ESATAN is then launched in Batch Mode from *Matlab*. The ESATAN-TMS graphical user interface is thus no more used than for geometry creation check and for radiative analysis.

The practical approach described here, essentially the coupled use of ESATAN-TMS and *Matlab*, is based on the work of Lionel Jacques [1], with a few exceptions as the use of the ESATAN-TMS interface to perform the radiative analysis.

The Figures 3.11 and 3.12 exemplify the knowledge available through this thermal modelling.

As a reminder, this section does not aim at performing a comprehensive thermal study of the battery system. This justifies the only display of exemplifying results.

A typical temperature profile used during cycling thermal tests is imposed to the system through its environment. This profile stays constant at 0°C during an hour before reaching a hot temperature of 20°C following a slope of $13.3^{\circ}\text{C}/\text{hour}$. This hot temperature is stabilised during another hour. These steps (slope of $13.3^{\circ}\text{C}/\text{hour}$ and stabilisation during an hour) are then repeated to successively reach 0°C and the cold temperature of -20°C . Finally, the environment temperature is lead back to 0°C .

Superimposed to this profile (depicted in red), the temperature of the cover and of a battery are given in Figure 3.11.

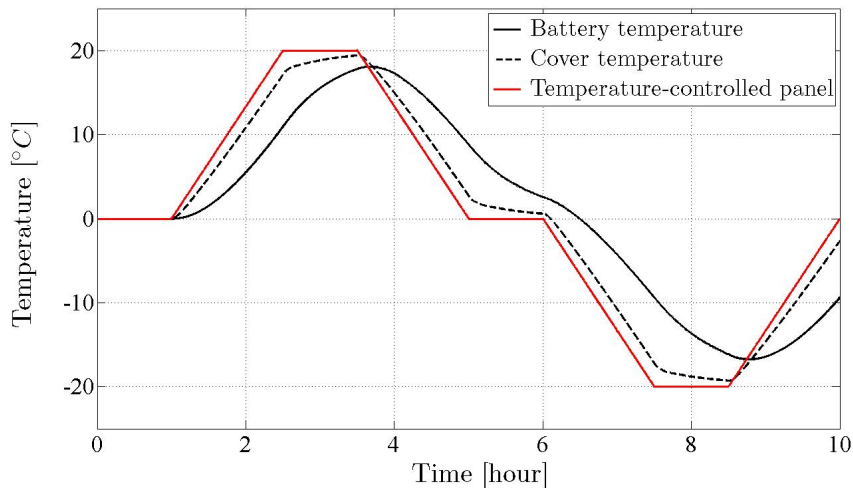


Figure 3.11: Thermal modelling results, given as an example

Two elements can be extracted from those curves. Firstly, the time-lag between the excitation (the imposed temperature profile) and the system response is a clear display of the importance of inertia within the system.

In addition, the second element to be noticed is the effect of the Polyester insulator wrapping the battery, in other words the effect of the absence of any conductive path to transport heat from or to that battery. This effect is visible through the important time-lag between the excitation and the battery temperature response, through the smoother behaviour of this response

curve compared to cover temperature curve and lastly through the lower temperature level reached (in hot and cold cases) by this response.

The Figures 3.12 and 3.13 display the radiative flux between the environment and the cover and between that cover and battery, respectively. The imposed temperature profile is also superimposed on those curves to enable a better understanding of flux transient behaviours.

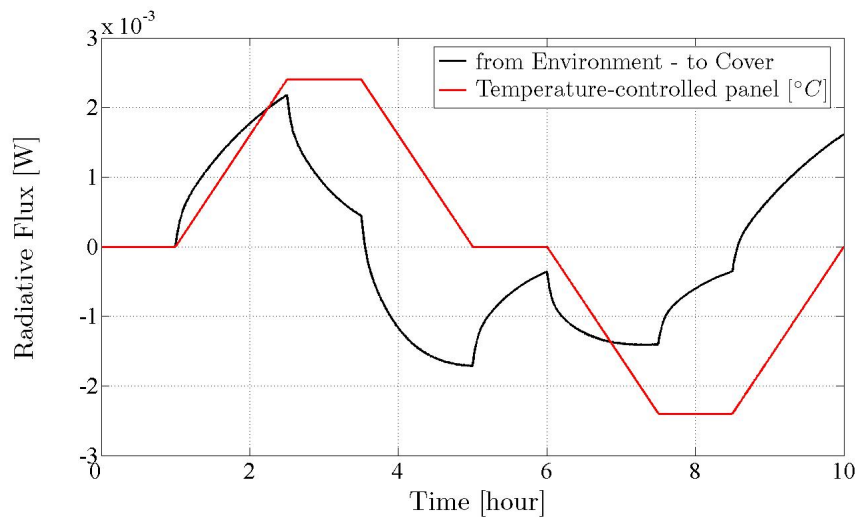


Figure 3.12: Thermal modelling results, given as an example (2)

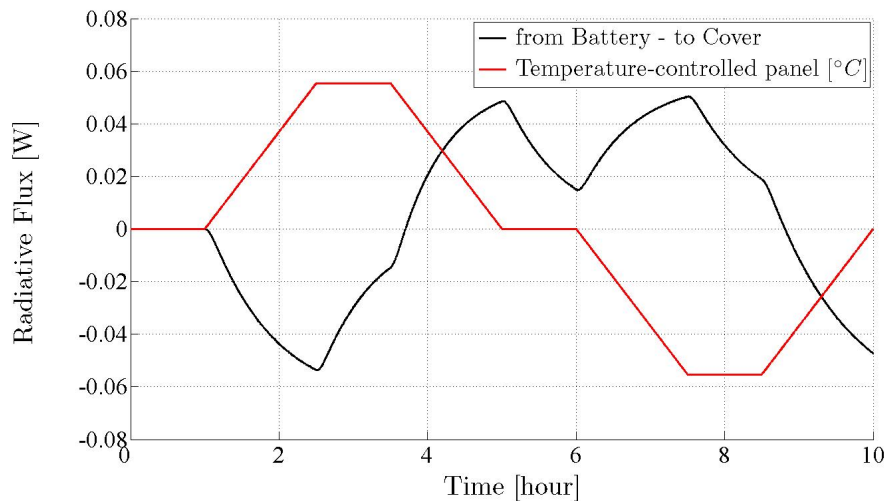


Figure 3.13: Thermal modelling results, given as an example (3)

It is interesting to see that, considering flux, each discontinuity of the imposed temperature profile derivative infers a simultaneous discontinuity in the response derivative. What's more, each environment stabilisation corresponds to a flux decrease, tending towards zero, the system containing no energy source.

3.2 Test procedure

The “ECSS-E-10-03A Space engineering: Testing” [8] distinguishes three major test categories, namely development testing, qualification testing and acceptance testing, defined as follows:

- Development testing: *“its objective is to support the design feasibility, to assist in the evolution of the design and to validate new design concepts and the application of proven concepts and techniques to a new configuration.”*
- Qualification testing: *“its objective is the formal demonstration that design implementation and manufacturing methods have resulted in hardware and software conforming to the specification requirements. The qualification testing will demonstrate that the items perform satisfactorily in the intended environments with sufficient margins.”*
- Acceptance testing: *“its purpose is to demonstrate conformance to specification and to act as quality control screens to detect manufacturing defects, workmanship errors, the start of failures and other performance anomalies, which are not readily detectable by normal inspection techniques.”*

Clearly, the test programme we intend to perform is a **development test**, also known as engineering test. Indeed, our aim is to validate the design concept largely detailed in previous sections, i.e. the use of mechanical thermostats and heaters as active control system, the choice to insulate the batteries from their direct environment and finally the design of reinforcers to cancel out under-vacuum deformations.

3.2.1 Test objectives

Gilmore [5] recalls that *“development test requirements are necessarily unique to the test objectives and are not specified in standards [...]”*

Indeed, as observed above, a development test is set up in order to help the design process of a given hardware component in providing an experimental information about its behaviour. This information is primarily used to detect potential problems during the design process and gives time to bring them solutions prior to beginning a formal qualification test.

Thus, it clearly appears that a well-considered objectives definition is essential in order to establish an efficient test procedure and to guarantee the relevancy of the recorded information.

Three main aspects of the battery system are likely to be tested and ultimately validated, namely:

- the battery system thermal behaviour.
- the battery system mechanical behaviour.
- the batteries electrical behaviour.

Thermal objectives

Clearly, the exhaustive validation of all the battery system thermal aspects is of utmost importance. Four thermal objectives can be enumerated:

1. to confirm the thermostats proper performance.
2. to prove that, in worst cases, the batteries temperature never exceeds its allowable range.
3. to provide data for thermal model correlation, taken during temperature transition (for transient correlation) and at equilibrium (for steady-state correlation).
4. to assess the impact of losing a heater on the system behaviour.

The thermostats proper performance validation includes the survey of their closing and reopening, and the certification of the conformity of these transitions with the corresponding batteries temperatures.

Mechanical objectives

The test mechanical objective is unique and evident (using a continuous numbering):

5. to prove that the support, in particular its reinforcers, and the cover do not undergo any failures due to batteries inflation and consequently that battery deformations are well arrested.

Electrical objectives

Objectives like testing and monitoring the batteries protection circuit or recording any battery characteristics are rejected in favour of thermal-related objectives.

Namely, they are:

6. to compute the energy consumption involves during a reheating phase.

7. to guarantee that, considering this consumption, the batteries voltage never drops below its minimal threshold of 2.7 V .
8. recording current and tension curves, to justify the choice of silver contact-thermostats according to the power involved.
9. to prove that the solution of cancelling out the under-vacuum deformations is adequate.

This objectives listing makes the writing of the thermal test procedure possible including, among other things, the imposed temperature curve within the vacuum vessel.

Before beginning this study, the next section describes in details all the elements necessary to set the test up.

3.2.2 Test setting up

In broad outline, the whole testing set-up is depicted in Figure 3.14. To consider as of now this sketch makes the reading of this section easier.

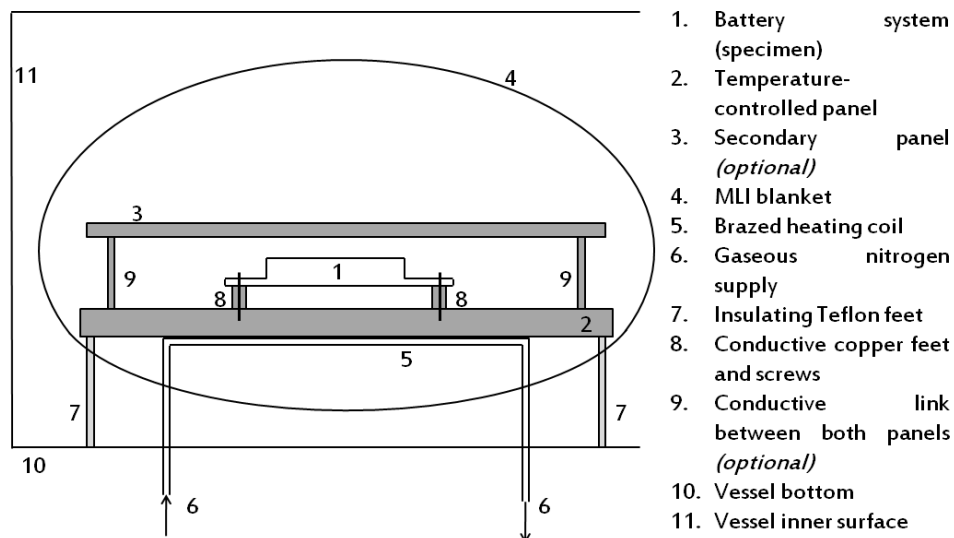


Figure 3.14: Testing set-up outline

Inside the vacuum vessel where the thermal test takes place, the temperature environment is regulated thanks to a temperature-controlled panel.

This panel is made up of copper because of its high thermal conductivity and thus its swift capability to make its temperature uniform. A heating coil, supplied in gaseous nitrogen, is generally brazed (that is to say metal-joined) on the rear side of this panel. The Figure 3.15 illustrates such an equipment.



Figure 3.15: The copper temperature-controlled panel (rear side) and the brazed heating coil

The gas supply is a mix of hot and cold gaseous nitrogen, the proportions of which are established to fit the temperature curve the experimenter wants to impose. Those two kinds of gas come from the same tank, the hot part being warmed up thanks to heaters under regulation automaton's control.

From a thermal point of view, the system to be tested (actually the batteries, the thermostats, the heaters and the insulator material integrated within the support and its cover) can be merely laid down on the temperature-controlled panel.

In this instance, the temperature profile imposed through that panel is transferred to the system by radiation only, because of the reduced importance of thermal conductive links in the vacuum ambience.

This fact raises a question. An important parameter to be assessed when defining a thermal testing procedure is the time constant of the system to be heated or cooled, that is an estimation of the time required to heat or cool the system from a given temperature. The question is: does this time stay reasonable?

The time constant can be computed as follows. Let us consider a system, initially at the temperature T_0 , dived in an environment at a lower (or equivalently higher) temperature T_{env} and study its transient behaviour. In other words, before the time $t = 0$, the system has the temperature T_0 and cools off afterwards whereas the environment temperature is of the form

$$T_{env} = T_0 H(-t) \quad (3.1)$$

where H is the Heaviside function.

Now, let us assume that the system temperature free decay is an exponential decay. Thus, this temperature decreases at a rate proportional to its value according to the relationship:

$$\frac{dT(t)}{dt} = -\lambda T(t) \quad (3.2)$$

whose solution is

$$T(t) = T_0 e^{-\lambda t} = T_0 e^{-t/\tau} \quad (3.3)$$

where λ is the decay constant whose inverse is the time constant τ .

Strictly speaking, the battery system we focus on does not exactly fulfil this assumption of exponential free decay. Such a free decay can only be rigorously demonstrated under specific assumptions [9]. The combining of conductive and radiative heat transfers prevents a rigorous demonstration.

However, that sinning of strictness is far from being detrimental since our aim is just a time constant estimation.

Then, the slope of the temperature curve in the neighbourhood of 0 directly gives τ , according to the Taylor series expansion

$$\frac{T(t)}{T_0} = e^{-t/\tau} = 1 - \frac{t}{\tau} + O(t^2), \quad t \cong 0 \quad (3.4)$$

Let us assess the time constant associated to the battery cooling process thanks to the thermal modelling developed in Section 3.1. To that purpose, a temperature decrease from $20^\circ C$ to $0^\circ C$ is imposed through the temperature-controlled panel, and one of the batteries' temperature is studied over a 48 hour period. This study is graphically displayed in Figure 3.16. The temperature drop imposed to the system is given in red whereas the black dotted line is the system's temperature free decay. The remaining black curve displays the free decay rate just after the temperature drop from which is deduced the system time constant.

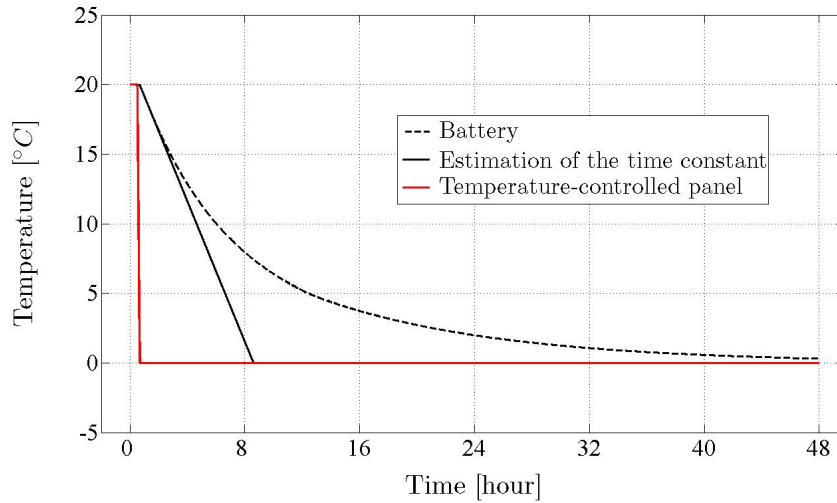


Figure 3.16: Time constant τ estimation of the battery cooling process

Following the foregoing developments and using the modelling developed in the previous section, the time constant can be computed and is found equal to 8 hours and 35 minutes. The Figure 3.16 even indicates that the battery finally reaches a temperature of $1^{\circ}C$ more than 28 hours after the drop of temperature within the vacuum vessel.

The necessity to enhance the heat transfer between the panel and the battery system is clear. The simplest way to accelerate that transfer is to screw the support on the panel to create, as well as a radiative link, an efficient conductive link. The most often, as that screwing, a SIGRAFLEX graphite foil is introduced between the panel and the specimen to be tested.

However, as developed below, mechanical aspect of the test demand to raise the height of the support with respect to the panel.

Those needs lead us to consider the links between the support and panel as four copper feet.

The Figure 3.17 illustrates the evolution of the time constant earlier introduced with an increasing conductive link between the battery support and the copper panel.

The existence if this thermal path rapidly make the time constant fall. Unfortunately, that decrease is limited to a value closed to 100 minutes. This reflects the limitation induced, for a given difference of temperature, by the heat transfer between the batteries and their environment solely carried out by radiation.

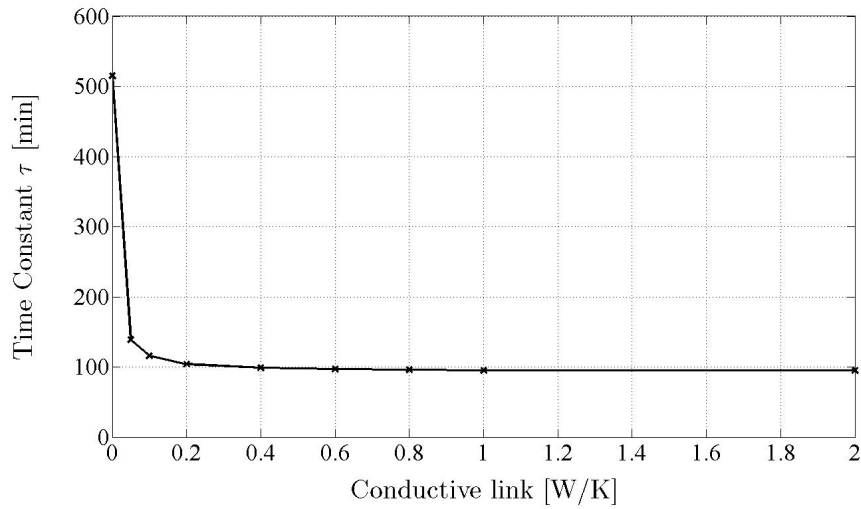


Figure 3.17: Relationship between the battery time constant τ and the importance of the thermal conductance between the battery support and the temperature-controlled panel

Indeed, the energy to be evacuated, from a battery to its environment — to decrease its temperature from 20°C to 0°C — is set by its thermal inertia. Thus, the necessary time for this evacuation is deduced from the importance of *ad hoc* radiative conductance.

So, no matter the magnitude of the conductive link studied in Figure 3.17, the cooling duration is limited by the saturation of that last thermal radiative path.

The set-up is completed by three last elements. The first of them is an optional second copper-panel, not supplied in nitrogen, facing the temperature-controlled panel and seeing the specimen with a view factor closed to one. What's more, if the need arises, it is linked to the main panel whose temperature is imposed through an efficient conductive link. Its purpose is again to enhance the radiative heat transfer to the system and to make that system temperature as closed as possible to the expected temperature profile. The system heat supply being provided through conductive links, this optional panel is not required.

Eventually, for the purpose of insulating, the last elements to be introduced are a Multi Layer Insulator (MLI) blanket (made up of ten Mylar layers) covering and closing up the whole thermal testing tent and Teflon

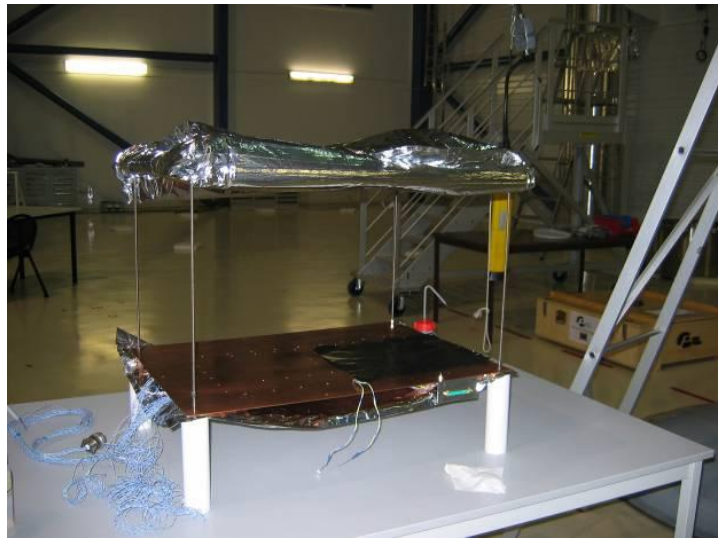


Figure 3.18: Copper temperature-controlled panel on insulating Teflon feet



Figure 3.19: Insulating MLI blanket covering up the whole set-up

feet cancelling out any thermal path between the temperature-controlled panel and the vessel bottom.

The two pictures given in Figures 3.18 and 3.19 enable a better visualization of the set-up. The copper temperature-controlled panel insulated from its support thanks to Teflon feet is displayed in Figure 3.18. The Figure 3.19 shows the MLI blanket used to entirely insulate the thermal testing tent. Both pictures are given by the way of illustration and correspond to a test

performed at the CSL on an electronic specimen.

The thermal set-up being completely defined, the temperature sensor positioning has lastly to be described. Two Pt-100 sensors will be placed on the copper panel to monitor and regulate the imposed profile of temperature. In addition, fifteen thermocouples will be distributed on the battery system to get the necessary information to the fulfilment of our thermal objectives, that is analytic correlation and hardware verification.

The Figure 3.20 illustrates the thermocouples positioning (red dots). The sensors numbered 3, 4 and 11-15 are arranged for the purpose of correlating the experimental results and the numerical model.

Just the opposite, the thermocouples 1, 2 and 5-10 will verify the hardware appropriate behaviour.

Thermocouples positioning and numbering are summarised in Table 3.1 to make the test setting up easier.

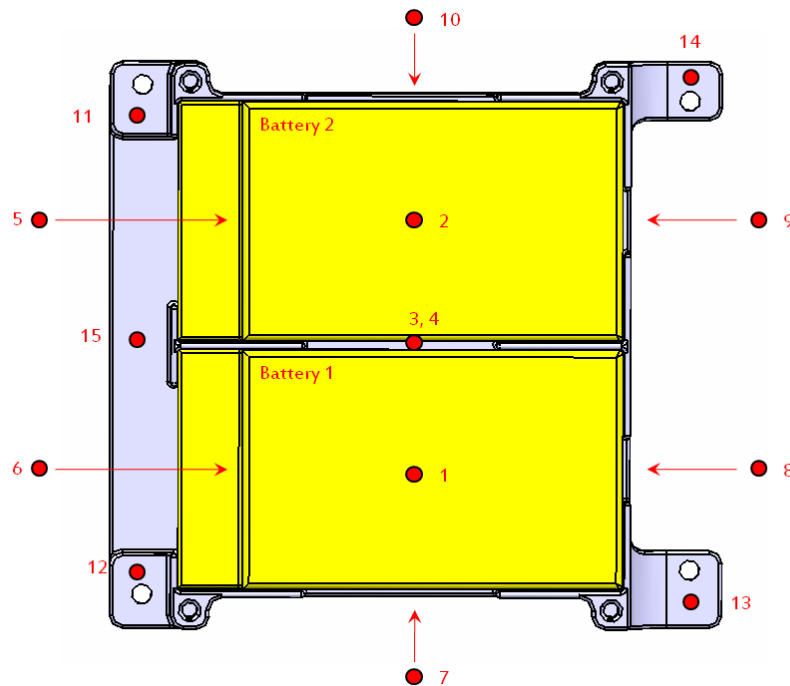


Figure 3.20: Thermocouples positioning and numbering (graphical display)

Thermocouple number	Position
1	Upon Battery 1, next to the thermostats
2	Upon Battery 2, next to the thermostats
3	Upon cover centre
4	Upon support centre, seen from underside
5	Upon Battery 2 lateral side, seen from the left in Figure 3.20
6	Upon Battery 1 lateral side, seen from the left
7	Upon Battery 1 lateral side, seen from the bottom
8	Upon Battery 1 lateral side, seen from the right
9	Upon Battery 2 lateral side, seen from the right
10	Upon Battery 2 lateral side, seen from the top
11	Upon support's top left corner
12	Upon support's bottom left corner
13	Upon support's bottom right corner
14	Upon support's top right corner
15	Upon support's middle left part

Table 3.1: Thermocouples positioning and numbering (summary)

Mechanical point of view

From a mechanical point of view, the only set-up requirement is to recreate at best the fixing system of the battery support in OUFTI-1 during the test process. This being so, the survey of possible cracks (plainly visible or not) in the support and its cover due to under-vacuum battery deformations will be realistic.

This leads, as already revealed above, to consider feet to raise the height of the battery support, still being screwed to the temperature-controlled panel through those feet. The crack detection method is outlined in Section 3.2.3.

Electrical point of view

The electrical information to be exchanged through the vacuum vessel wall, as well as the thermocouple measurements, consists of current and tension measures. In addition, an electrical link has to open the possibility, if need be, of recharging the batteries to simulate the solar cells power provision brought during sunshine periods.

The whole wiring will be concentrated through a dedicated Sub-D connector to leave the vessel further on.

The Figure 3.21 draws a diagram of this wiring including the batteries, the heaters (resistances), the thermostats (switches), the current and tension measurement devices and the recharging systems.

The maximum and minimum current and tension characteristics involved within this electrical scheme are dictated by the batteries and the heaters. They are brought together in Table 3.2.

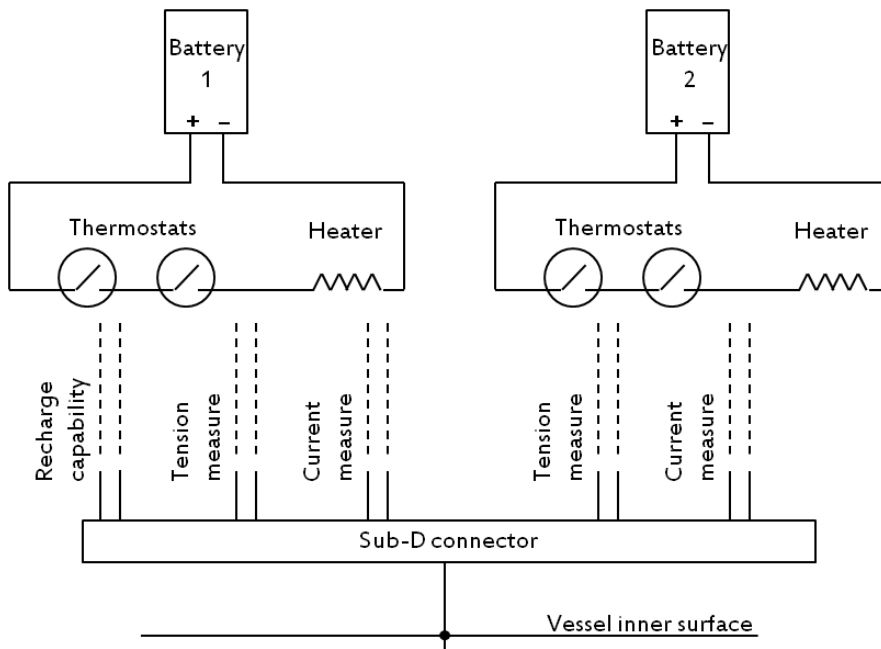


Figure 3.21: Test electrical set-up

	Minimum	Maximum
Current [mA]	0	160
Tension [V]	2.7	3.7

Table 3.2: Electrical set-up maximum and minimum characteristics (current and tension)

3.2.3 Test procedure

This last section dedicated to battery system validation process discusses the establishment of the test procedure itself. Its purpose is to describe the necessary stages to meet the nine test objectives in the framework of the setting-up outlined above.

The description of the thermal test, actually a thermal balance test, follows the outline of the crack detection method given below.

Crack detection method

Most of the listed test objectives will be fulfilled thanks to the survey of time series recorded during the thermal test, for instance temperature time series or current time evolution.

The objectives number 5 and 9 involve some actions before and/or after this test, though.

First, the ninth objective demands to demonstrate that the choice to force the battery not to deform is relevant. This proof will be brought by the anticipated batteries capacity good behaviour. A post-testing autopsy-like examination could also be envisaged to ascertain their integrity.

The objective 5 besides involves actions before and after the test. Indeed, if cracks appear within the support or the cover inside the vacuum vessel, they will cause changes in their stiffness properties essentially, but also in their mass and damping properties.

It arises from this observation that changes in structure dynamic features (natural frequencies, mode shapes, FRF peak characteristics) will become visible. Dynamic investigations such as sine swept or shock testing are likely to be efficient to identify such defects. According to STRU subsystem, a sine swept test process will be performed.

Thus, after clamping the support and then the cover on a shaker, the survey of the first natural frequencies before and after the test would highlight any cracks underwent under vacuum. That justifies the interest showed in the dynamic behaviours of the support and its cover in the section 2.3., independently from the whole mechanical system.

More information about the application of this detection procedure is to be found in [6]. The absence of a detailed description in this work is

justified by the delinking of the crack detection process from the thermal test itself. To be comprehensive, in-depth discussions about the content of non-destructive crack identification methods using dynamic properties can be found in Owolabi, Swamidas and Seshadri [10], Chondros and Dimarogonas [11] or Silva and Gomes [12].

Thermal Balance Test

According to Gilmore [5], a thermal balance test, performed in the framework of a development thermal testing programme, “*has two objectives: obtaining thermal data for analytic thermal model correlation and verifying the thermal control subsystem [...]*.”

Gilmore adds: “*Equilibrium temperatures or repeatable heater cycling profiles are typically the thermal data that are taken during the test. Verification of the thermal control subsystem includes performance verification of thermal hardware, including heaters, thermostats [...]*.” This definition clearly matches our objectives through the notions of cycling profiles and thermal hardware verification.

The cycling profile tailored to the battery system problem qualitatively consists of different stages. Starting from an ambient temperature, a decrease to a cold ambience followed by a symmetric temperature increase will control the proper performance of the mechanical thermostats and meet the objective 1. These stays in worst thermal conditions will also verify the second objective. The electrical objectives 6, 7 and 8 verification also results from this simple temperature profile. Finally, to meet the fourth objective, the cycling can be identically repeated while disconnected one of the heaters, thus simulating its loss.

Quantitatively, let us consider an initial ambient temperature of 20°C , maintained during 10 minutes to stabilize and initiate the thermal cycling. Thus, a cold temperature level, standing for an eclipse period, is reached through a given transition phase. Its duration is fixed to 40 minutes, that is to say an overestimation of the OUFTI-1 eclipse duration (slightly longer than 35 minutes). Then, the imposed hot temperature level simulates a permanently illuminated orbit, the time-length of which is set equal to 110 minutes (the orbit period being equal to 104 minutes).

The temperature transitions are chosen linear with a slope of 1.5 K/min , standing for an intermediate value. Indeed, a lower value would lengthen the test duration while a higher one (1.5 K/min being lower than the maximum reachable rate within the vessel) would not enhance the batteries response fastness, as observed above.

The last parameters to be defined are the hot and cold temperature levels to be imposed. On this point, Gilmore [5] writes: “*Where practical, development tests should be conducted over a range of operating conditions that exceed the design limits to identify marginal capabilities and marginal design features.*” According to [1], the batteries environment is supposed to undergo temperatures going from -15°C to 40°C . Then, setting margins of 10°C , the two cycles outlined here will spread over a 75°C interval, from -25°C to 50°C .

The thermal modelling developed in Section 3.1. is now exploited in order to simulate the thermal balance test. Two simulation curves are displayed in Figures 3.22 and 3.23.

In Figure 3.22, the imposed temperature profile is depicted in red. The batteries responses (as seen from the thermocouples 1 and 2) are given in black (continuous and dotted lines). The dotted line stands for the battery whose heater is turned off during the second cycle.

The Figure 3.23 depicts the system response as seen from the thermocouples 3 and 4 (cover and support main sides). For the sake of clarity and in order to enable an efficient use during the test, those two graphs are enlarged, anti-clockwise rotated and annotated.

The Table 3.3 completes the information given in Figures 3.22 and 3.23 through a thorough listing of the thermal balance test major events, along with their respective time, given in seconds. What’s more, for each recorded time, the imposed temperature is reported enabling a clear numerical definition of this profile.

The last two columns display the duration of each quoted phase, in seconds then in minutes.

Lastly, some events are reported in Table 3.3 in italic. They indicate minor events essentially related to the batteries temperature behaviour. Those events are not counted in the duration columns.

I would finally describe these two graphs through a limited number of commentaries.

Principally, the effect of the insulation between the batteries and their neighbourhood is to be noticed. Indeed, the delay of the batteries response to the imposed profile along with its smoother progression clearly highlight the presence of an insulator material and the resulting unique radiation heat

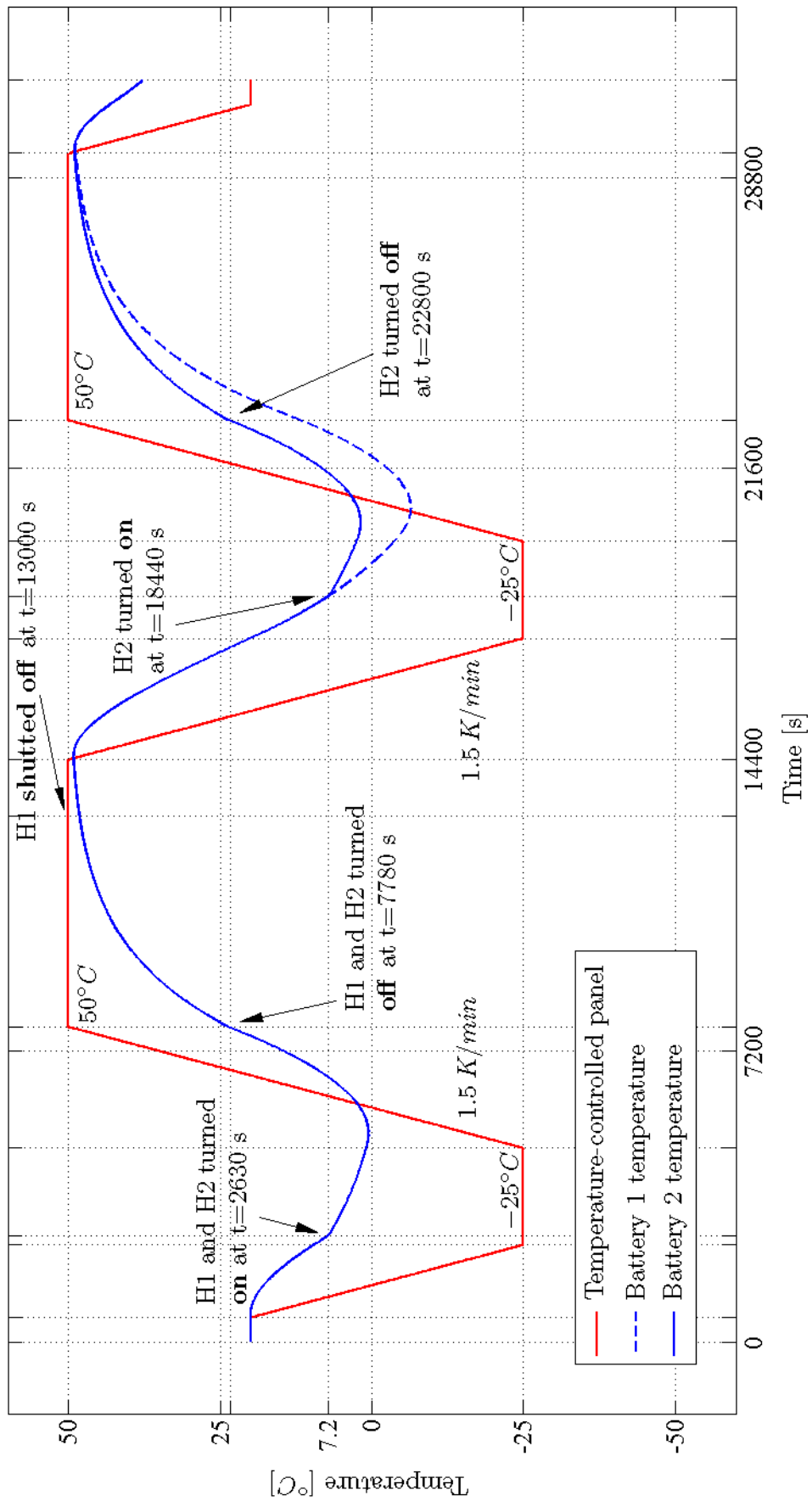


Figure 3.22: Test simulation as seen from the batteries thermostats-side

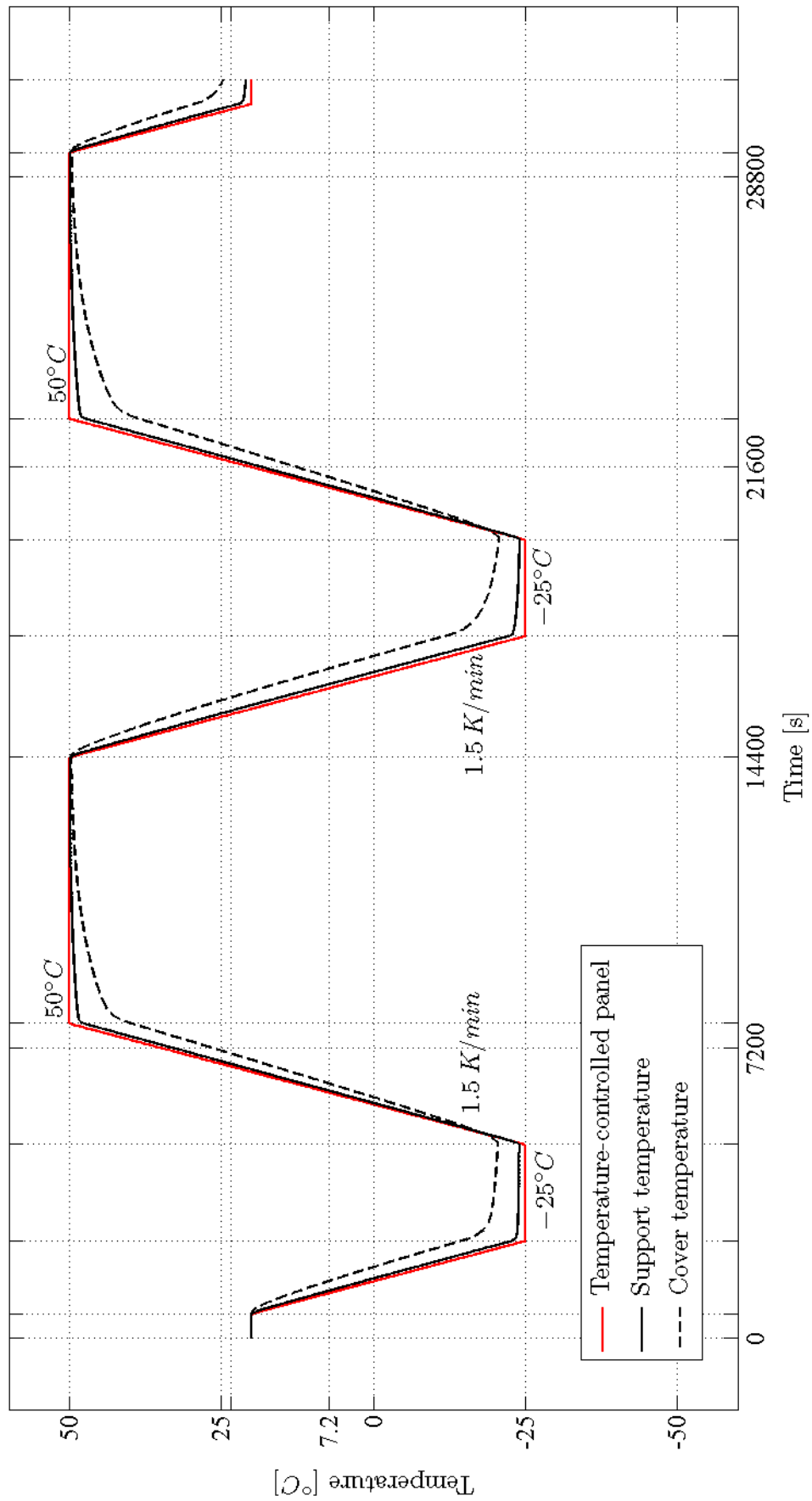


Figure 3.23: Test simulation as seen from the support and the cover

Time in seconds	Imposed temperature profile [$^{\circ}C$]	Event	Duration in seconds	Duration in minutes
0	20	Test start and beginning of initialization phase ($20^{\circ}C$)		
600	20	End of initialization phase and beginning of transition phase ($1.5 K/min$)	600	10
2400	-25	Cold level start ($-25^{\circ}C$)	1800	30
2630	-25	Heaters 1 and 2 turning on	230	3.83
4800	-25	End of cold level and beginning of transition phase ($1.5 K/min$)	2170	36.17
5120	-17	<i>Batteries minimal temperature - $0.52^{\circ}C$</i>	-	-
7780	49.5	Heaters 1 and 2 turning off	2980	49.67
7800	50	Hot level start ($50^{\circ}C$)	20	0.33
9770	50	<i>Batteries temperature overrides $40^{\circ}C$</i>	-	-
13000	50	Heater 1 shutting off	5200	86.67
14400	50	End of hot level and beginning of transition phase ($1.5 K/min$)	1400	23.33
14450	48.75	<i>Batteries maximum temperature - $49.14^{\circ}C$</i>	-	-
17400	-25	Cold level start ($-25^{\circ}C$)	3000	50
18440	-25	Heater 2 turning on	1040	17.33
19260	-25	<i>Battery 1 temperature drops below $0^{\circ}C$</i>	-	-
19800	-25	End of cold level and beginning of transition phase ($1.5 K/min$)	1360	22.67
20250	-13.75	<i>Battery 2 minimum temperature - $1.83^{\circ}C$</i>	-	-
20610	-4.75	<i>Battery 1 minimum temperature - $-6.46^{\circ}C$</i>	-	-
22800	50	Hot level start ($50^{\circ}C$) and Heater 2 turning off	3000	50
24880	50	<i>Battery 2 temperature overrides $40^{\circ}C$</i>	-	-
25480	50	<i>Battery 1 temperature overrides $40^{\circ}C$</i>	-	-
29400	50	End of hot level and beginning of transition phase ($1.5 K/min$)	6600	110
29480	48	<i>Battery 1 maximum temperature - $48.83^{\circ}C$</i>	-	-
29480	48	<i>Battery 2 maximum temperature - $49.01^{\circ}C$</i>	-	-
30600	20	End of transition phase and beginning of stabilization phase	1200	20
31200 = 8h 40 min	20	Test end	600	10

Table 3.3: Test progression, imposed temperature and major and minor test events along with their durations

transfer.

Another illustration of the insulating material effect is the lesser influence of the heaters switching on or off on the support and cover temperature curves. This influence can however be underlined in Figure 3.23, through the observation of the gap between the imposed temperature and the support (or the cover) response in cold case. This gap reflects the power generated by the heaters and disappears in hot case.

Furthermore, the absence of any steady-state phase has to be pointed out. This leads to the failure to comply with our third objective which demands to obtain correlation data during equilibrium phases. Nevertheless, this lack is acceptable in order to shorten the test duration even if it makes the correlation more complex.

In addition, when defining the hot and cold temperature levels to be reached during the thermal balance test, the purpose of identifying marginal capabilities and marginal design features was followed. Those features can be seen in Figure 3.22. Thus, the batteries temperatures surpassing their 40°C threshold, the 86-minute first reheating phase or the not heated battery temperature drop below 0°C stand for system marginal features or capabilities.

At last, it is central to point out that the considered temperature profile does not stand for worst cold case conditions, as undergone by the battery system. Indeed, the choice of 50°C hot temperature level runs counter to a worst cold case definition.

Because of this lack of representativeness, the thermal test outlined here is unable to certify the battery system thermal requirements, that is the objective 2. Anyway, the closeness between the blue temperature curve and the 0°C critical limit in Figure 3.22 makes impossible the inference of the design validity.

Nevertheless, the test keeps a considerable interest since it will improve the numerical modelling capability to determine the thermal design relevancy and will open the way for other test programmes.

3.3 Conclusions

The third chapter of this dissertation intended to gather the necessary tools to validate the design described in the previous chapter.

Those tools, introduced and developed in this chapter, are namely:

- a comprehensive definition of the validation test objectives. To obtain data for model transient correlation and to certify the thermostats proper performance are the two main objectives of the thermal validation test. Other objectives were envisaged but finally rejected, because of test duration considerations essentially.
- a detailed description of the test set-up. The main questioning about this set-up was the thermal link to be used to heat or cool the battery system. Conductive links turned out to be ideals.
- a test procedure designed to underline the listed objectives. This test is a thermal balance test consisting of two symmetric cycles, ranging from a -20°C cold temperature level to a 50°C hot level.
- a thermal modelling of the battery system to assess parameters such as its time constant or to ultimately simulate the validation procedure.

Chapter 4

Minor issues

To introduce this last chapter, here are other extracts of L. Jacques's work's conclusion:

“ Concerning the hot case, the dissipation system developed by EPS subsystem was the cause of nearly all issues: involving too high temperatures on the batteries and the dissipation transistor. To solve these problems, drastic measures had to be taken in order to reduce temperature.”

“ The third issues occurring in the hot case involves the COM amplifier [...]”

This chapter intends to evaluate the technical situation of these two minor thermal issues.

It should be emphasized that, because of many uncertainties that still surround their complete definition, the settlement of those two issues is not achieved in this work. However, as soon as the required information will become available, the outlined solutions will shortly be materialised.

4.1 The dissipation transistor in hot case

The exceeding power generated by the solar panels and dissipated through the EPS transistor is not so much an issue for the transistor itself as the temperature rise experienced by its environment.

Two solutions were envisaged [1]. The first one consists in shunting a part of the energy to be dissipated directly to the antennas panel through resistances. The use of two $4.7\ \Omega$ resistances in parallel is required, preventing the transistor from depolarizing.

Beyond this first solution, a strap, encircling the transistor, is also required to reach an acceptable level of temperature within its neighbourhood. This strap is supposed to drain off heat from the EPS PCB to the antennas panel again. Numerical information demonstrate that both solutions are strictly necessary.

The tasks to be completed in order to definitely solve this problem are namely:

- to assess the thermal conductance needed to drain the excessive heat off. This calculation assumes the knowledge of (1) the minimal difference of temperature between the transistor and the antennas panel and (2) the dissipated power.
- to design and manufacture an appropriate strap, considering the conductance computed before and the available space on the EPS PCB, that is to say to choose its material and geometry.
- to deal with the questions of thermal interface conductance and electrical insulation.

The transistor exact dissipated power is still unknown. The EPS subsystem however envisions testing the solar panels-shunt-transistor system to access this piece of information.

Because of its high thermal conductivity, the choice of a strap made up of copper is planned except if, because of drastic mass constraints, a compromise between a high thermal conductivity and a low density has to be reached.

Furthermore, the quality of the thermal interface conductance is to be reached by screwing the strap on the EPS PCB as well as on the antennas panel. In addition, thermo-conductive resin, actually Stycast 2850FT (also used to glue the mechanical thermostats on the batteries), has to be inserted between both surfaces to guarantee an effective thermal path.

Lastly, it is of central importance to consider the electrical link created by the strap between the EPS PCB and the antennas panel and its consequences. On one hand, this link between an electronic component and the earthed antennas panel could be detrimental. On the other hand, it is advised against completely insulating the strap, at the risk of creating electric potential gradients and electrostatic shocks.

4.2 The COM amplifier in hot case

In the conclusion of his work [1], L. Jacques writes: *“The third issues occurring in the hot case involves the COM amplifier, because of its quite low efficiency and therefore high heat dissipation. No concrete measures have been taken to solve this problem because too many uncertainties still surround its definition.”*

In March 2010, I wrote in a document summarizing the state of OUFTI-1 thermal issues: *“The power dissipated by the COM amplifier is foreseen as being a potential issue. However, this power is far from being definitely known, and this issue is thus let in abeyance.”* [13]

Since then, the situation did not evolve. To the best of my knowledge, the amplifier project is not materialised yet. This leads to a lack of information mainly concentrated around its dissipated power and its location.

Furthermore, the two main conclusions brought last year thanks to numerical simulations [1] are that:

- of course, the less dissipative amplifier the better. For instance, a 1.75 W dissipative amplifier would produce 45°C hot spots within its PCB (compared with the PCB’s mean temperature) while a 0.5 W dissipative amplifier would produce 15°C hot spots.
- according to numerical simulations again, a middle edge location for the amplifier would constitute the worst choice.

The COM subsystem is advised of this possible and detrimental heat generation, and is conscious that the easiest solution to this potential problem is simply to try not to meet it. Thus, the possibility to opt for a low-dissipative amplifier not located in the middle of the PCB edges is shared by COM subsystem.

Yet, if the need arises to settle a too high temperature level draining excessive heat off, certainly not so much an issue for the amplifier itself than for its environment, a copper-strap, as envisaged for the EPS dissipation transistor, is worthwhile being firstly considered. It would connect the amplifier with the antennas panel again. The question of its location upon the COM PCB may thus become central.

Considering this location and the available space on the COM PCB, the possibility of a flexible thermal strap has not to be ruled out.

Moreover, its conductance would be simply assessed knowing the minimal difference of temperature between the antennas panel and the amplifier, and the power to be evacuated, two unavailable pieces of data up to now.

Lastly, it should be emphasized that interface conductance and electrical insulation will anyhow demand attention.

Chapter 5

Conclusions

Ideally, this thesis should have proposed a last chapter dedicated to the results of the test programme outlined in chapter 3. Unfortunately, the battery system validation, to be performed at the CSL, is scheduled for the end of June.

This dissertation essentially dealt with the OUFTI-1 battery issue. This issue was first stated, considering its thermal, mechanical and electrical aspects. Making reference to the work carried out last year, a review of the unresolved problems and design inconsistencies was conducted. The complete design of the battery system naturally resulted from this statement.

In chapter 2, the design of a complete active thermal control system of the batteries was proposed, involving, per battery:

- one heater — the source of energy.
- two mechanical thermostats in series — the reheating decision-making mechanism.
- an electrical power supply, that is to say the battery itself.
- two Polyester netting layers — the energy wasting reduction devices.

In addition, the battery system support, that is to say the mechanical aspect of the problem, was reviewed to settle an available space issue and to cancel out the battery under-vacuum deformations.

A comprehensive thermal modelling of the whole system was developed in chapter 3. It subtends the definition of the validation test procedure largely detailed at the end of this chapter. The test objectives and test setting up were firstly considered prior to establishing a complete and appropriate test

procedure.

The dissertation ended with the review of the technical state of the two minor thermal issues of OUFTI-1.

I eventually want to list the main tasks of the OUFTI-1 Thermal Control Subsystem that still have, according to me, to be completed:

1. to perform the test programme defined in this dissertation and to process the recorded data.
2. to correlate the thermal modelling of the battery system and the experimental results and to assess untested system behaviours.
3. if necessary, to tailor the design proposed in this work to the validation procedure results.
4. to integrate the thermal model outlined in this work in the global modelling developed last year.
5. to define, conduct and post-process the thermal validation tests of OUFTI-1.

Bibliography

- [1] L. JACQUES. Thermal design of the oufti-1 nanosatellite. Master's thesis, University of Liège, 2009.
- [2] J. P. W. STARK P. W. FORTESCUE and G. G. SWINERD. *Spacecraft Systems Engineering - Third Edition*. John Wiley and Sons Ltd, 2003.
- [3] C. J. M. Verhoeven and W. J. Ubbels. Delfi-C³, past, present and future, 2008.
- [4] P. LEDENT. Vacuum tests for varta and kokam batteries. Technical report, University of Liège, 2009.
- [5] D. G. GILMORE. *Spacecraft Thermal Control Handbook. Volume I: Fundamental Technologies*. The Aerospace Press, 2002.
- [6] N. FRANCOIS. Dynamic analysis and launch qualification of oufti-1 nanosatellite. Master's thesis, University of Liège, 2010.
- [7] P. ROCHUS. *Conception d'Expériences Spatiales*. University of Liège, 2010.
- [8] ESA Publications Division. ECSS-E-10-03A : Space engineering - testing. European Space Agency, 2002.
- [9] J. H. LIENHARD IV and J. H. LIENHARD V. *A Heat Transfer Textbook*. Phlogiston Press, Cambridge, Massachusetts, U.S.A., 2008.
- [10] A. S. J. Swamidas G. M. Owolabi and R. Seshadri. Crack detection in beams using changes in frequencies and amplitudes of frequency response functions. *Journal of Sound and Vibration*, 2002.
- [11] T. G. Chondros and A. D. Dimarogonas. Vibration of a cracked cantilever beam. *Journal of Vibration and Acoustics*, 1998.
- [12] J. M. M. Silva and A. J. M. A. Gomes. Experimental dynamic analysis of cracked free-free beams. *Journal of Experimental Mechanics*, 1994.
- [13] J.-P. NOËL. Thermal issues and solutions - synthesis. Technical report, OUFTI-1 CubeSat, University of Liège, 2010.

Appendix 1

This Appendix first displays the first five eigenmodes of the battery support, the first five eigenmodes of the cover coming next. Two views are proposed per eigenmode, from the points of view considered in Figure 5.1.

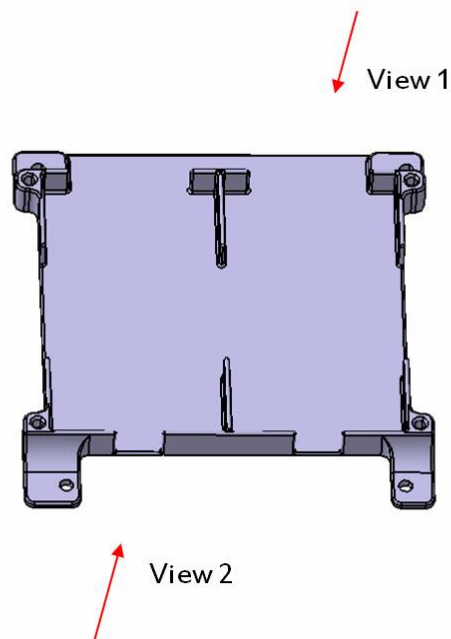


Figure 5.1: Display of the support and the cover eigenmodes

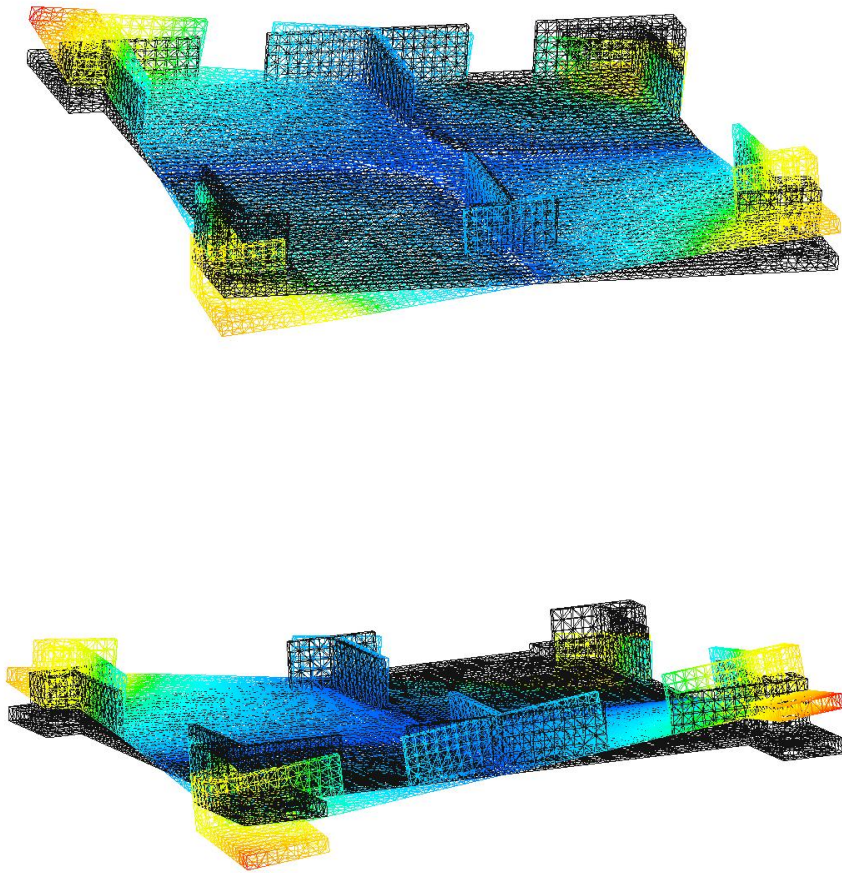


Figure 5.2: The battery support: First eigenmode – 733 Hz

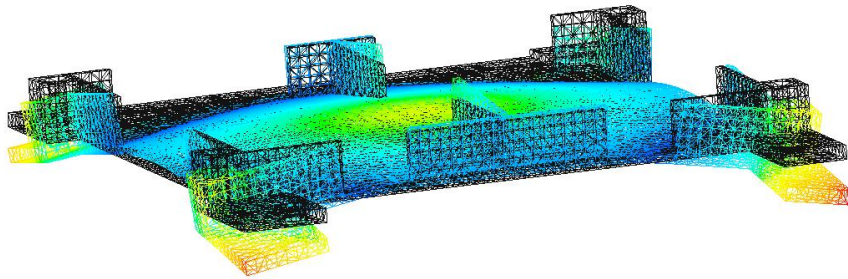
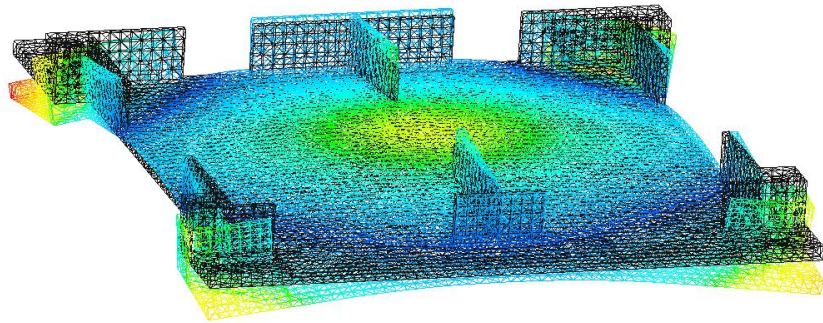


Figure 5.3: The battery support: Second eigenmode – 1219 Hz

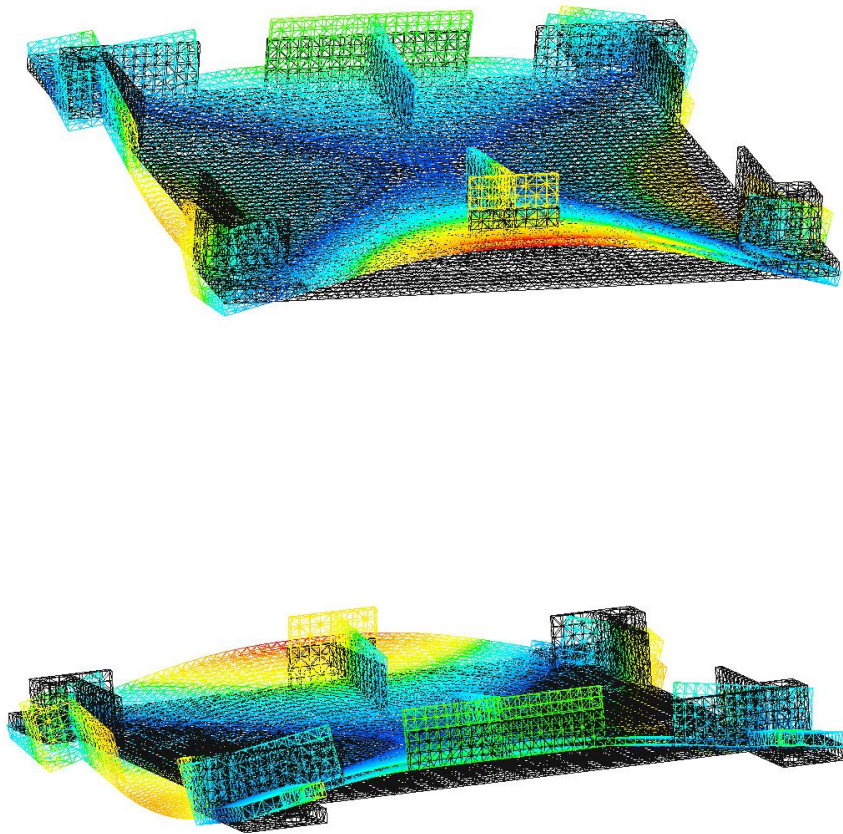


Figure 5.4: The battery support: Third eigenmode – 1434 Hz

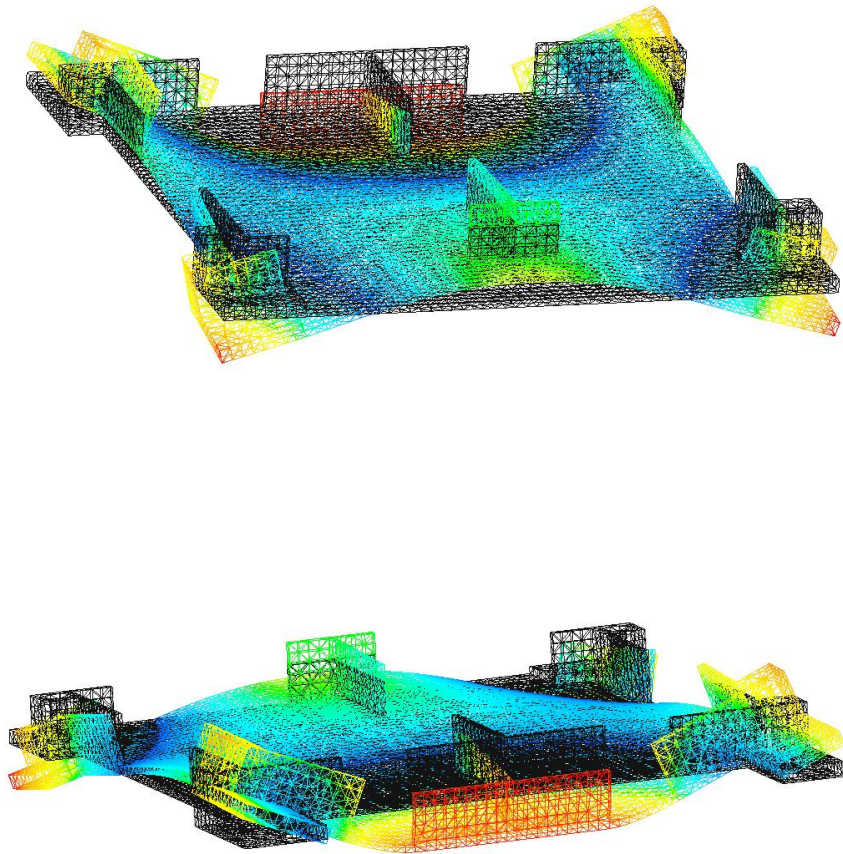


Figure 5.5: The battery support: Fourth eigenmode – 1787 Hz

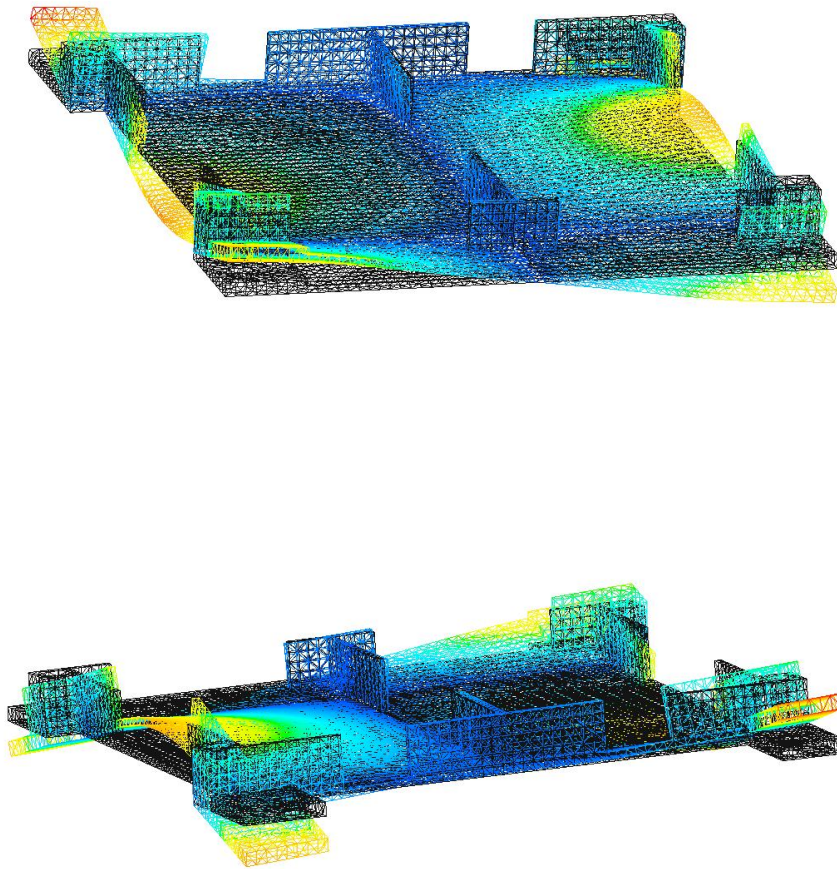


Figure 5.6: The battery support: Fifth eigenmode – 2102 Hz

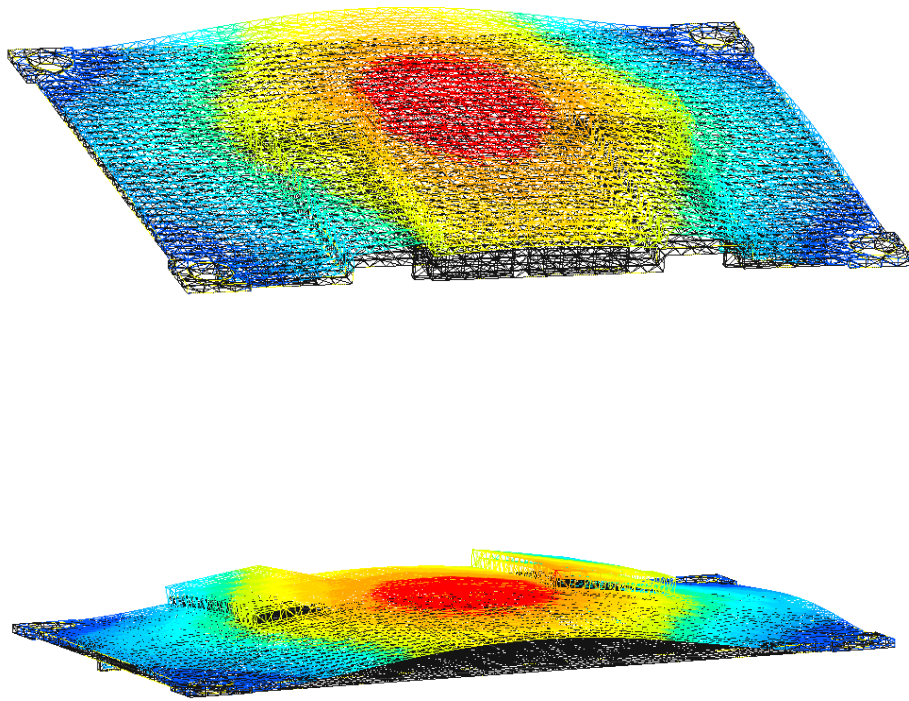


Figure 5.7: The cover: First eigenmode – 1460 Hz

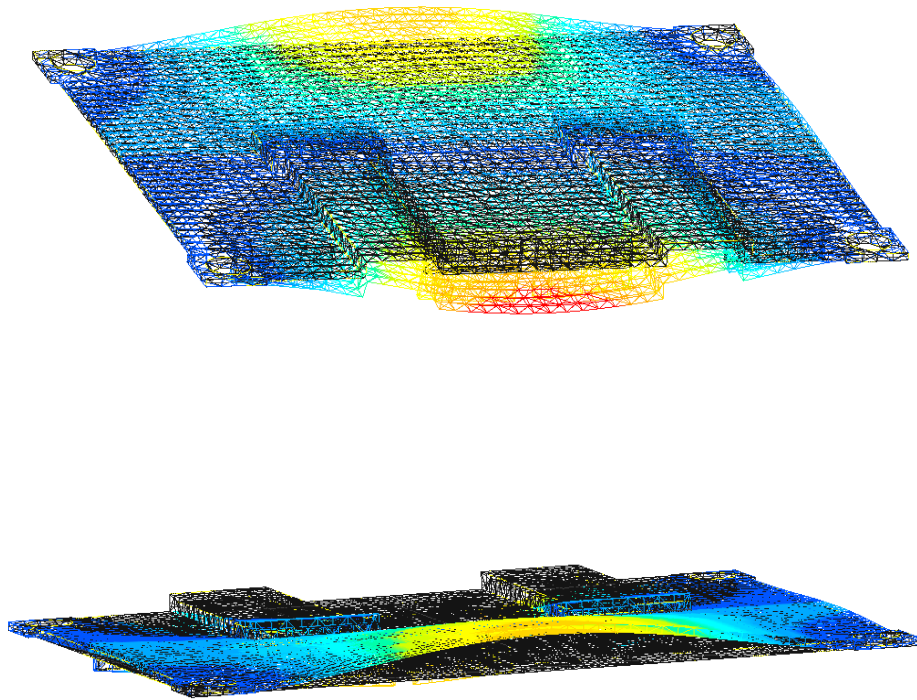


Figure 5.8: The cover: Second eigenmode – 2826 Hz

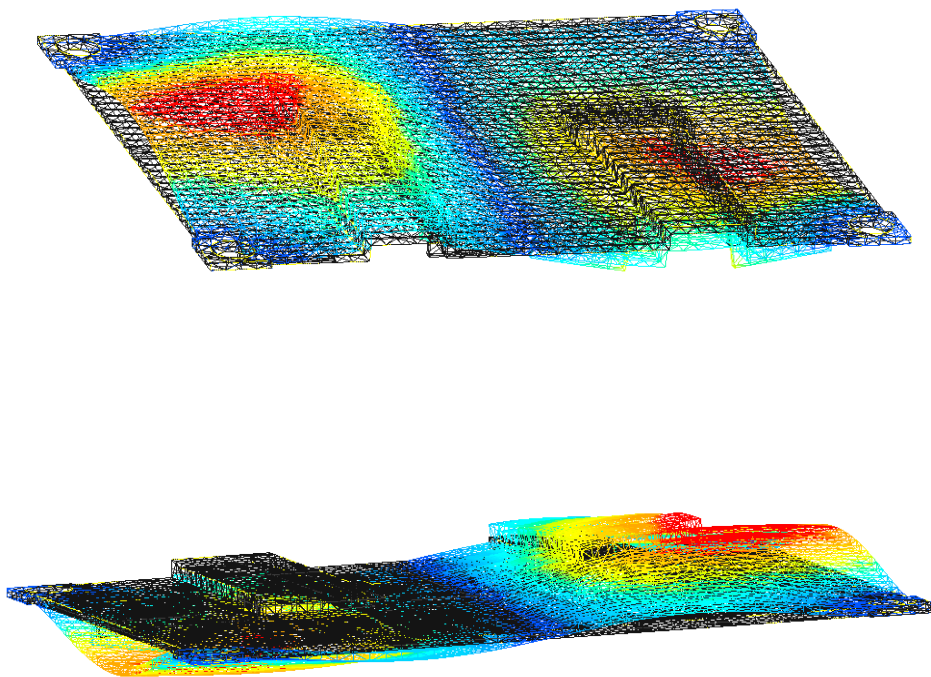


Figure 5.9: The cover: Third eigenmode – 3254 Hz

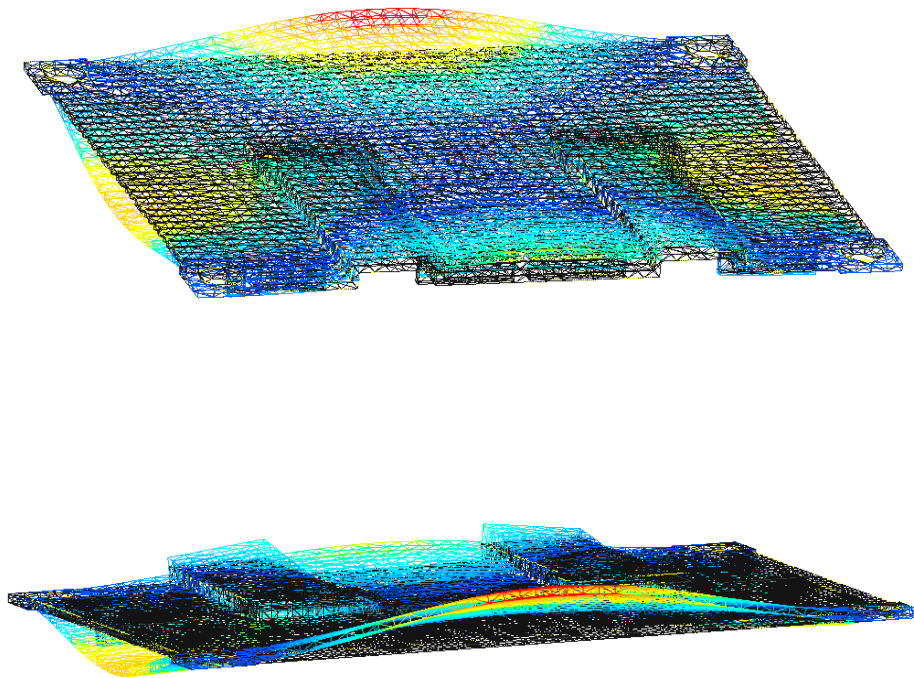


Figure 5.10: The cover: Fourth eigenmode – 3773 Hz

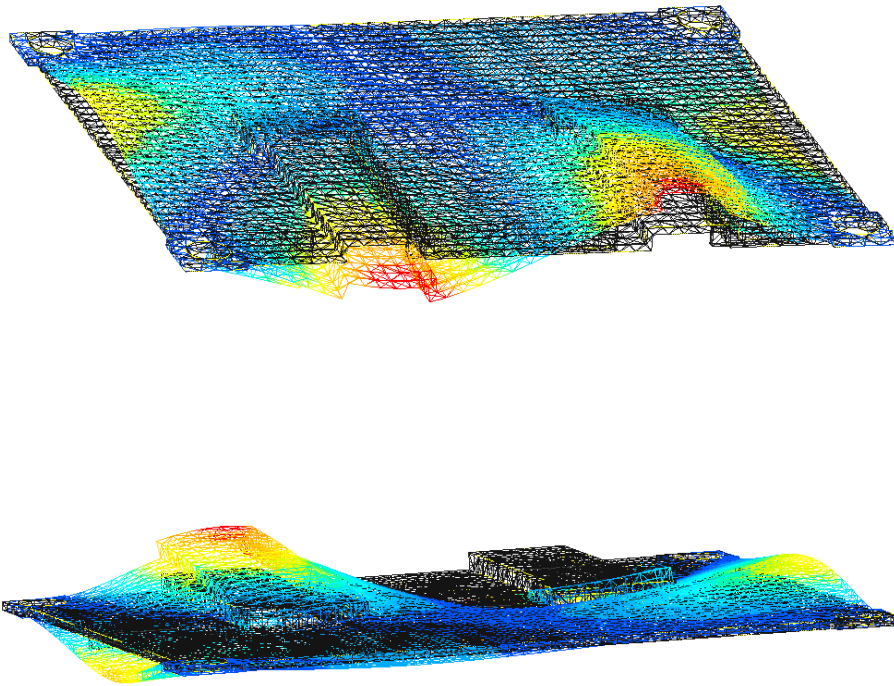


Figure 5.11: The cover: Fifth eigenmode – 5493 Hz

Appendix 2

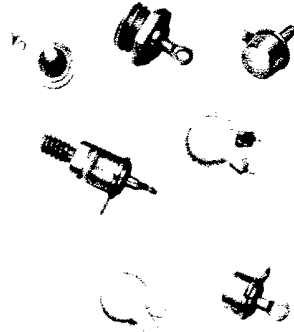
This second Appendix gathers the datasheets of every hardware component mentioned in this work.

The following datasheets are successively displayed:

- (4 pages) the Klixon Tiny Stat Miniature Thermostats Series, in which lies the 4BT-2 model, obtained from the manufacturer.
- (1 page) the Stycast 2850FT Epoxy resin, taken from the ECSS-Q-70-71A: *Space product assurance - Data for selection of space materials and processes*.
- (2 pages) the MINCO Thermofoil Heaters, obtained from the manufacturer.
- (2 pages) the SHELDAHL Polyester Netting, obtained from the manufacturer.
- (2 pages) the KOKAM SLB 603870H Battery, obtained from the manufacturer.

3BT & 4BT Series Tiny Stat Miniature Thermostat

- Smallest snap-acting thermal switches ever made
- Qualified to MIL-S-24236/13 & /19, Type 1, Class 4 (order by MS number)
- Extremely fast response
- Single pole, single throw
- Normally open or normally closed
- Pre-set, non-adjustable calibration
- Various mounting configurations available
- Hermetically sealed and back-filled with nitrogen
- GAM - T1



Actual size

Military

Description

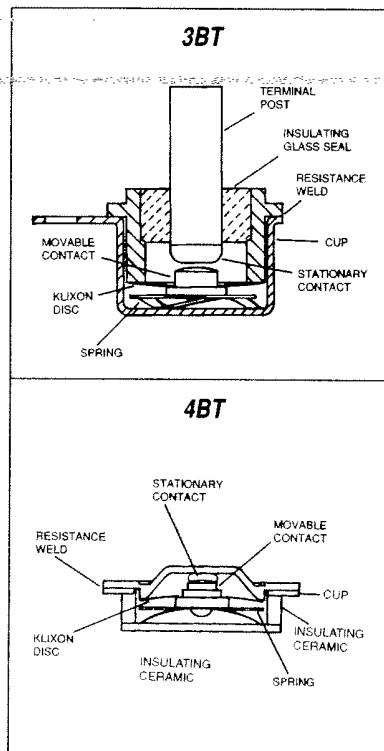
Tiny-Stat miniature thermostats combine an impressive list of superlatives in a reliable, hermetically-sealed, snap-acting Klixon design. They are the smallest envelope size ever developed – ideal for remote sensing applications in locations having severe space limitations. They are the lightest construction available for applications where weight is an important consideration. They have extremely fast response to permit early warning of overheat conditions and their low mass internal components allow Tiny-Stat miniature thermostats to meet the most demanding standards of MIL-S-24236 for shock and vibration.

Gold plated contacts can be furnished for the electrical loads listed in the following table to assure reliable circuit switching under low wattage conditions. Gold plated contacts are not suitable for higher loads.

Gold Contact Ratings (Resistive)

30 VAC/DC	500 mA and below
115 VAC	200 mA and below

Typical Cross-Section View



Switching Action

All thermostats are supplied with single pole, single throw switching. The contacts can be constructed as:

Normally closed - limit type application, contacts open on temperature rise at a pre-determined temperature to de-energize the circuit. Contacts automatically re-close as the device cools to a pre-determined temperature.

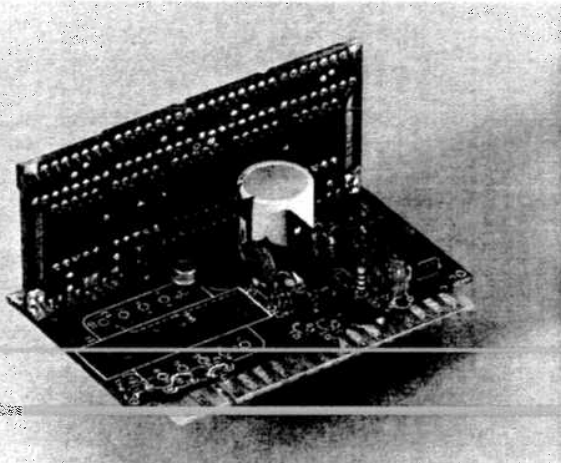
Normally open - fan type application, contacts close on temperature rise at a pre-determined temperature to de-energize the circuit. Contacts automatically re-open as the device cools to a pre-determined temperature.

The opening and closing temperatures are pre-set and non-adjustable.

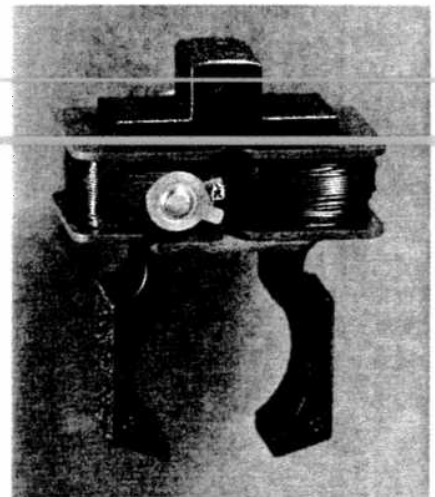
Common Applications

The Tiny Stat® Thermostats afford the user the quality and performance of a Klixon® Thermostat in a sub-miniature package. Tiny Stats® are the smallest snap-acting thermal switches ever made which makes them the ideal choice in applications where *size* and *weight* are critical. This small envelope design translates to a low thermal mass which yields one more key feature, an *extremely fast thermal response*.

Tiny Stats® are commonly used . . .

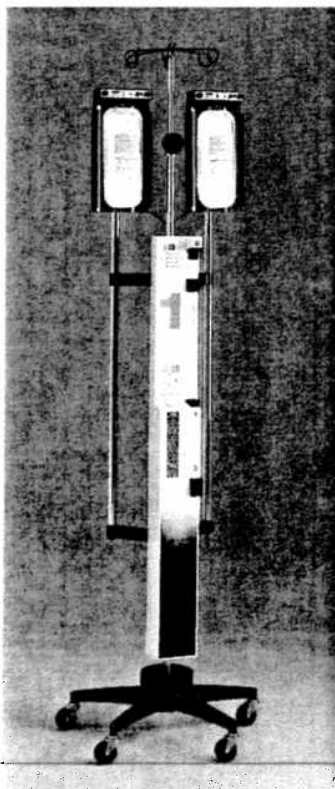


. . . for electronics overheat protection. The 3BT-15 configuration is printed circuit board mountable. Other configurations can be epoxied in place.



. . . in transformer windings. The low profile design of the 4BT-2 is optimal for this application.

. . . in medical equipment. Where rapid thermal response is paramount, the Tinystat® is the solution.



Performance Characteristics

Switch Action

SPST (snap-action)

Contact Resistance

0.050 ohms maximum

per MIL-STD-202, Method 307

0.100 ohms maximum for close on rise devices with setpoints greater than 175°F

**Contact Ratings (Resistive)
10,000 Cycles**

Voltage	115VAC/ 30VDC	30mVAC*	30mVDC*
Amperes	1.0 (silver contacts)	0.01	0.01

Based on standard differential

*Specify gold contacts

Dielectric Strength

500 VAC, rms, 60 cycles for 1 min., across open contacts, per MIL-STD-202, Method 301

Vibration Resistance

5-2000 Hz, 30G, per MIL-STD-202, Method 204

Shock Resistance

100G, 6 milliseconds, per MIL-STD-202, Method 213

Hermeticity

1 X 10⁻⁸ atm cc/sec. max., per MIL-STD-202, Method 112, Condition C

Salt Spray

per MIL-STD-202, Method 101, Condition B, 5% solution

Weight

Basic unit 0.2 to 0.9 grams

* Devices which open on temperature rise should not be subjected to vibration while at temperatures of 75°F or more below the opening temperature.

Devices which close on temperature rise should not be subjected to vibration while at temperatures of 75°F or more above the closing temperature.

Temperature (Use table below for common operating temperatures).

Ambient Temperature Range:

-80°F to +350°F, (-62.2°C to 176.7°C)

Operating temperature

Temperature at which normally closed contacts open or normally open contacts close.

Tolerance

Allowable range above and below setpoint and reset temperatures.

Differential

Subtract the differential from the operating temperature to determine the temperature at which the contacts will return to the normal position (reset temperature).

Dash #	Oper. Temp.		Differential		Tolerance	
	°F	°C	°F	°C	±°F	±°C
1	0	-17.8	30	16.7	8	4.4
2	5	-15.0	30	16.7	8	4.4
3	10	-12.2	30	16.7	8	4.4
4	15	-9.4	30	16.7	8	4.4
5	20	-6.7	30	16.7	8	4.4
6	25	-4.0	30	16.7	8	4.4
7	30	-1.1	30	16.7	8	4.4
8	35	1.7	30	16.7	8	4.4
9	40	4.4	30	16.7	8	4.4
10	45	7.2	30	16.7	8	4.4
11	50	10.0	30	16.7	8	4.4
12	55	12.8	30	16.7	8	4.4
13	60	15.6	30	16.7	8	4.4
14	65	18.3	30	16.7	8	4.4
15	70	21.1	30	16.7	8	4.4
16	75	23.9	30	16.7	8	4.4
17	80	26.7	30	16.7	8	4.4
18	85	29.4	30	16.7	8	4.4
19	90	32.2	30	16.7	8	4.4
20	95	35.0	30	16.7	8	4.4
21	100	37.8	30	16.7	8	4.4
22	105	40.6	30	16.7	8	4.4
23	110	43.3	30	16.7	8	4.4
24	115	46.1	30	16.7	8	4.4
25	120	48.9	30	16.7	8	4.4
26	125	51.7	30	16.7	8	4.4
27	130	54.4	30	16.7	8	4.4
28	135	57.2	30	16.7	8	4.4
29	140	60.0	30	16.7	8	4.4
30	145	62.8	30	16.7	8	4.4
31	150	65.6	30	16.7	8	4.4
32	155	68.3	30	16.7	8	4.4
33	160	71.1	30	16.7	8	4.4
34	165	73.9	30	16.7	8	4.4
35	170	76.7	30	16.7	8	4.4
36	175	79.4	30	16.7	8	4.4

Dash #	Oper. Temp.		Differential		Tolerance	
	°F	°C	°F	°C	±°F	±°C
37	180	82.2	30	16.7	8	4.4
38	185	85.0	30	16.7	8	4.4
39	190	87.8	30	16.7	8	4.4
40	195	90.6	30	16.7	8	4.4
41	200	93.3	30	16.7	8	4.4
42	205	96.1	30	16.7	8	4.4
43	210	98.9	30	16.7	8	4.4
44	215	101.7	30	16.7	8	4.4
45	220	104.4	30	16.7	8	4.4
46	225	107.2	30	16.7	8	4.4
47	230	110.0	30	16.7	8	4.4
48	235	112.8	30	16.7	8	4.4
49	240	115.6	30	16.7	8	4.4
50	245	118.3	30	16.7	8	4.4
51	250	121.1	30	16.7	8	4.4
52	255	123.9	30	16.7	8	4.4
53	260	126.7	30	16.7	8	4.4
54	265	129.4	30	16.7	8	4.4
55	270	132.2	30	16.7	8	4.4
56	275	135.0	30	16.7	8	4.4
57	280	137.8	30	16.7	8	4.4
58	285	140.6	30	16.7	8	4.4
59	290	143.3	30	16.7	8	4.4
60	295	146.1	30	16.7	8	4.4
61	300	148.9	30	16.7	8	4.4
62	305	151.7	30	16.7	8	4.4
63	310	154.4	30	16.7	8	4.4
64	315	157.2	30	16.7	8	4.4
65	320	160.0	30	16.7	8	4.4
66	325	162.8	30	16.7	8	4.4
67	330	165.6	30	16.7	8	4.4
68	335	168.3	30	16.7	8	4.4
69	340	171.1	30	16.7	8	4.4
70	345	173.9	30	16.7	8	4.4
71	350	176.7	30	16.7	8	4.4

Consult factory if desired operating temperature does not appear in the table.

Standard Configurations

Many standard configurations are available including pin type terminals for quick assembly to printed circuit boards (3BT-2 and 3BT-15), threaded plug for surface temperature sensing (3BT-3), and

an insulated version for applications where grounded case construction is not suitable (3BT-6). The 4BT-2 is designed specifically for applications where an extremely low profile is critical.

Part Numbering System for Standard 3BT & 4BT Thermostats

4BT L 2 - 22 - 98

TYPE
3BT or 4BT

L = Open on rise silver contacts

R = Open on rise gold contacts

F = Close on rise silver contacts

D = Close on rise gold contacts

STYLE

STANDARD OPERATING TEMPERATURES
#1 through 71 starting at 0°F in 5°F increments
Reset 30°F lower

OPTIONAL WIRE LEAD FOR 4BT
Teflon* insulated, 12" long

98 - Stranded, fig. A
103 - Solid, fig. B

(Others available)
Omit if leads are not required.

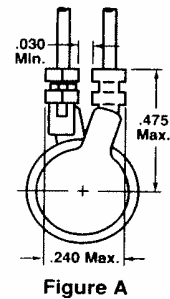
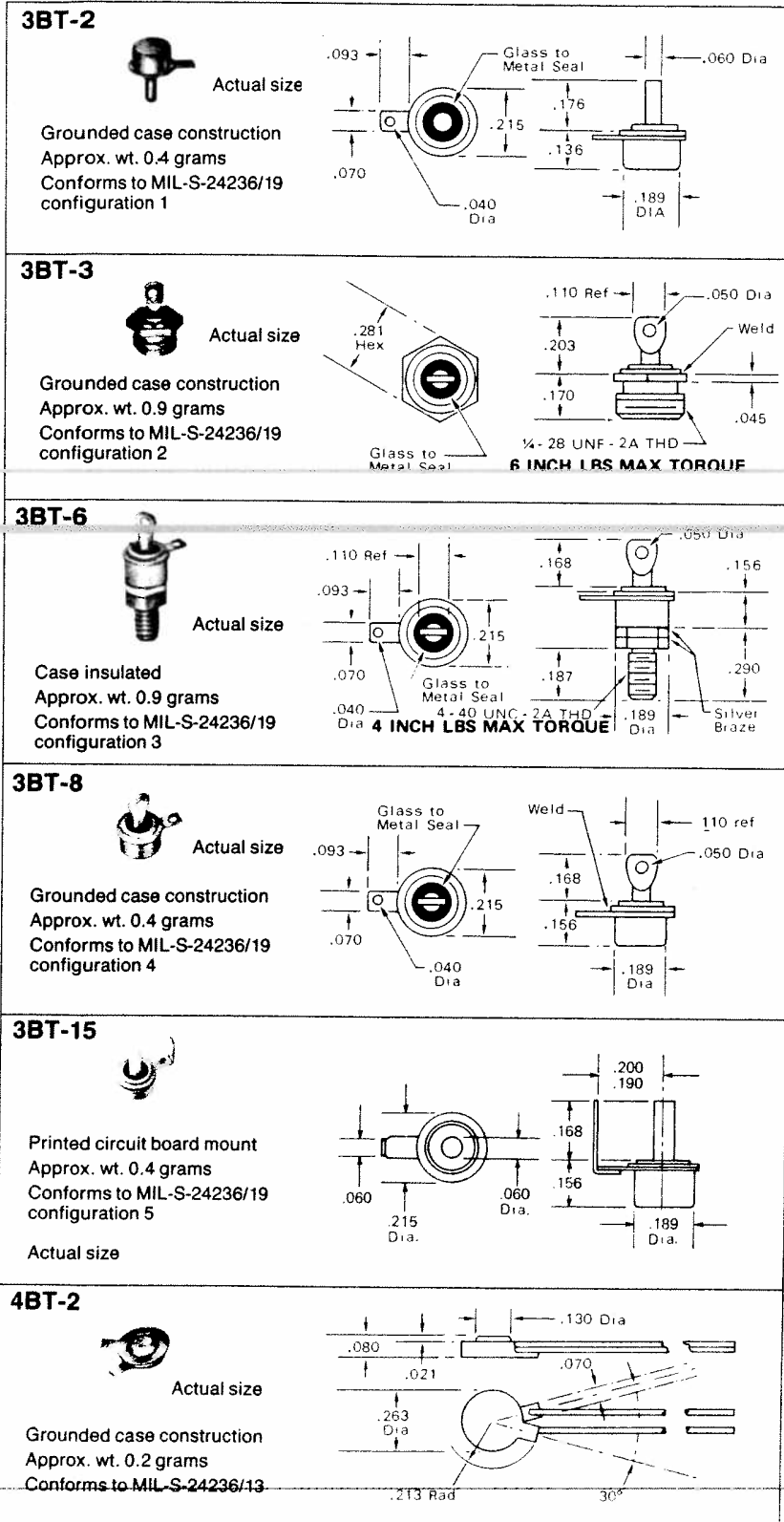


Figure A

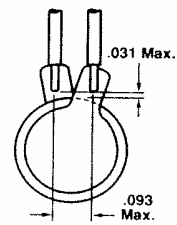


Figure B

All dimensions nominal, in inches.

* Trademark of E.I. DuPont de Nemours and Co.

C.14.12 Stycast 2850FT

PRODUCT

Type	2-part potting resin.	
Chemical Composition	Epoxy.	
Manufacturer	Emerson & Cumming	Tel: +32 14 56 25 00
	Nijverheidsstraat 7,	Fax: +32 14 56 25 01
	B-2260 Westerlo	Email:
	Belgium	www.emersoncumming.com

EXPERIENCE and AVAILABILITY

Development Status	Commercial Product
Cost Range	Low
Lot Reproducibility	Excellent
Space Experience	Extensive

GENERAL PROPERTIES (Physical, Mechanical, Thermal, Electrical, Optical)

Nature	Typical Value	Remarks
Specific Gravity	2,3	Manufacturer's Data
Viscosity (before reaction)	70 000 cps	Manufacturer's Data
Pot Life	45 min	Manufacturer's Data
Hardness	94	Shore D
Tensile Strength	60 MPa	Manufacturer's Data
Compressive Modulus	80 MPa	Manufacturer's Data
Thermal Expansion Coefficient	$29 \times 10^{-6} \text{ } ^\circ\text{C}^{-1}$	Manufacturer's Data
Thermal Conductivity	$1,44 \text{ W m}^{-1} \text{ } ^\circ\text{C}^{-1}$	@ 25 °C
Electrical Resistivity (volume)	$5 \times 10^{12} \text{ } \Omega \text{ m}$	@ 25 °C
Dielectric Constant	6,5	@ 60 Hz.
Loss Factor	0,02	@ 60 Hz.
Dielectric Strength	15 kV/mm	Manufacturer's Data

PROPERTIES RELEVANT TO SPACE USE

Nature	Typical Value	Type of Test
Temperature Range	Up to 205 °C	Manufacturer's Data
Outgassing	TML = 0,38 %, RML = 0,24 %, CVCM = 0,01 %	ECSS-Q-70-02
Oxygen Index	29,8	ECSS-Q-70-21
Toxicity/Offgassing	Pass	NASA-STD-6001
Water Absorption	< 0,15 %	Over 7 days
Flammability	Pass (23,8 % O ₂)	NASA-STD-6001

SPECIAL RECOMMENDATIONS

- Recommended cure is 24 hours at room temperature, plus 4 hours at 60 °C with catalyst 9.
- Other catalysts are available for the same resin, but these affect the properties: Catalyst 11 for high-temperature cure; Catalyst 24 LV for low viscosity. Some experience in space is available for both.
- A derived resin (2 850 KT) can be used for extremely high thermal conductance ($4,2 \text{ W m}^{-1} \text{ } ^\circ\text{C}^{-1}$).

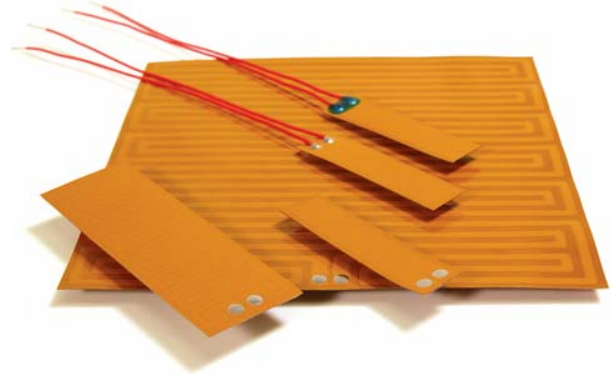
Commercial Grade Polyimide Heaters

Reliable heating options at an affordable price

Overview

Minco's commercial grade polyimide heaters provide the performance and reliability you expect at a lower cost than our standard polyimide/FEP models. Sizes are available for 12 and 24 volt operation, or connect multiple heaters in a series/parallel system for consistent power over larger areas.

- Solder pad option provides you the lowest price possible for Minco polyimide heaters
- All models include acrylic pressure sensitive mounting adhesive (PSA) for simple installation
- Ideal for prototyping, short production series or high volume/low cost applications
- Typical lead time is 3-5 days ARO



Commercial grade polyimide heaters

Polyimide Heaters

Specifications

Temperature range: -32 to 100°C .

Material: Polyimide film/acrylic (Kapton™ or equivalent).

Resistance tolerance: ±10%.

Minimum bend radius: 0.030" (0.8 mm).

Electrical connection options: Exposed solder pads. Options include two AWG 26 PTFE insulated leadwires 4" (100 mm) long with insulated or bare connection points.

Specification options

HK5950	Base model from table
L	Termination options:*
	S = Solder pads
	L = 4" (100 mm) PTFE insulated leadwires - lead attachment area not insulated
	P = 4" (100 mm) PTFE insulated leadwires with insulated connection points
HK5950L = Sample part	

*Due to solder junctions parts are not RoHS compliant

Insulated connection wire for end-user attachment

Order loose insulated connection wires with stripped ends for fast, easy connection of heaters to your power source. These AWG 26 wires have high temperature PTFE insulation resistant to wear and abrasion. The insulation color is red and the standard length is 4" (100 mm). Wires are sold in pairs, order one pair for each heater. Order part number AC102371.

Base model table

Model numbers	Size (inches)	Size (mm)	Resistance in ohms	Voltage	Watt density W/in ² (W/cm ²)	Effective area in ² (cm ²)
HK5950	0.5 x 2.0	12.7 x 50.8	57.5	12	2.5 (0.39)	1.0 (6.45)
HK5951	1.0 x 1.0	25.4 x 25.4	57.5	12	2.5 (0.39)	1.0 (6.45)
HK5952	0.5 x 5.0	12.7 x 127	23.0	12	2.5 (0.39)	2.5 (16.13)
HK5953	1.0 x 3.0	25.4 x 76.2	19.2	12	2.5 (0.39)	3.0 (19.35)
HK5954	2.0 x 2.0	50.8 x 50.8	57.6	24	2.5 (0.39)	4.0 (25.81)
HK5955	3.0 x 3.0	76.2 x 76.2	25.6	24	2.5 (0.39)	9.0 (58.06)
HK5956	4.0 x 4.0	101.6 x 101.6	14.4	24	2.5 (0.39)	16.0(103.2)
HK5957	5.0 x 5.0	127 x 127	9.2	24	2.5 (0.39)	25.0 (161.29)

Specifications subject to change



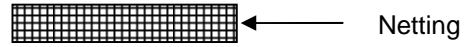
Standard Polyimide and Rubber Heaters

Size (in)		Size (mm)		Type	Resistance options- ohms*						Effective area in ² (cm ²)	Lead AWG	Insu- lation	Model number	
X	Y	X	Y		R(0°C) [May be used with Heaterstat] → NiFe Ni										
1.22	2.24	31.0	56.9	8	111	55.5	29.5	14.8	9.8	7.4	17.2	2.33 (15.03)	30	K, R	5368
1.23	2.48	31.2	63.0	2	101	50.8	27.1	13.5	9.4	6.7	15.7	2.60 (16.77)	30	K, R	5369
1.24	1.80	31.5	45.7	2	298	148	90.1	43.3			46.2 10.6	1.90 (12.26)	30	K	5370
1.25	1.25	31.8	31.8	21	100	52.2	28.4	13.1	9.7	7.3	15.5	1.42 (9.16)	30	K, R	5587
1.25	1.50	31.8	38.1	21	125	65.3	35.5	16.4	12.2	9.2	19.4	1.71 (11.03)	30	K, R	5588
1.25	1.75	31.8	44.5	21	150	78.4	42.6	19.7	14.6	11.0	23.3 5.3	2.01 (12.97)	30	K, R	5589
1.25	6.30	31.8	160.0	1	136	68.2	41.3	19.8	13.6	9.5	21.1	6.84 (44.13)	24	K, R	5371
1.25	8.80	31.8	223.5	1	51.9	25.9	15.7	7.5	5.1	3.6	8.0	9.86 (63.61)	24	K, R	5372
1.25	15.00	31.8	381.0	1	219	109	66.5	32.1	21.9	15.3	33.9 7.6	15.79 (101.87)	24	K, R	5373
1.35	5.60	34.3	142.2	3	876	438	265	127			136 31.1	6.57 (42.39)	30	K	5374
1.37	5.80	34.8	147.3	1	250	125	75.8	36.5	24.9	17.5	38.8 8.7	7.15 (46.13)	26	K, R	5375
1.38	2.75	35.1	69.9	2	305	152	92.1	44.2			47.3 10.8	3.21 (20.71)	26	K, R	5376
1.40	2.34	35.6	59.4	1	197	98.7	52.5	26.3	17.5	13.1	30.5 6.9	2.90 (18.71)	30	K, R	5377
1.40	6.30	35.6	160.0	8	771	386	205	103			120 27.2	8.08 (52.13)	30	K, R	5378
1.45	2.40	36.8	61.0	8	106	53.4	32.3	15.5	10.6	7.4	16.4	2.90 (18.71)	26	K, R	5379
1.45	8.15	36.8	207.0	8	474	237	126	63.1	42.1	31.5	73.5 16.6	10.52 (67.87)	24	K, R	5380
1.48	10.10	37.6	256.5	1	126	62.9	33.5	16.7	11.2	8.4	19.5	13.40 (86.45)	24	K, R	5381
1.50	1.50	38.1	38.1	21	150	78.3	42.6	19.7	14.6	11.0	23.3 5.3	2.07 (13.35)	30	K, R	5590
1.50	1.75	38.1	44.5	21	175	91.4	49.7	23.0	17.1	12.9	27.1 6.2	2.43 (15.68)	30	K, R	5591
1.50	2.00	38.1	50.8	1	14.8	7.2	4.5					1.84 (11.87)	24	K, R	5382
1.50	3.00	38.1	76.2	1	21.8	10.7	6.6					3.14 (20.26)	24	K, R	5383
1.50	4.00	38.1	101.6	1	29.1	14.4	8.8	4.3				4.44 (28.65)	24	K, R	5384
1.50	4.10	38.1	104.1	2	103	51.7	27.5	13.7	9.2	6.9	16.0	4.00 (25.81)	30	K, R	5385
1.50	5.00	38.1	127.0	1	36.2	17.9	10.9	5.1	3.4		5.6	5.74 (37.03)	24	K, R	5386
1.50	6.00	38.1	152.4	1	43.3	21.7	13.2	6.2	4.2		6.7	7.04 (45.42)	24	K, R	5387
1.50	6.42	38.1	163.1	8	140	70.2	37.4	18.7			21.7	7.70 (49.68)	30	K, R	5388
1.50	6.42	38.1	163.1	8	1317	659	350	175			204 46.8	8.50 (54.84)	30	K, R	5389
1.50	7.00	38.1	177.8	1	50.1	25.1	15.2	7.2	4.7	3.5	7.8	8.34 (53.81)	24	K, R	5390
1.50	8.00	38.1	203.2	1	57.1	28.7	17.5	8.1	5.3	3.9	8.9	9.64 (62.19)	24	K, R	5391
1.50	8.05	38.1	204.5	2	304	152	92.1	44.3	30.3	21.2	47.1 10.6	10.80 (69.68)	26	K, R	5392
1.50	9.00	38.1	228.6	1	64.1	32.2	19.6	8.9	6.1	4.4	9.9	10.94 (70.58)	24	K, R	5393
1.50	10.00	38.1	254.0	1	71.4	35.7	21.8	10.1	6.7	4.9	11.1	12.24 (78.97)	24	K, R	5394
1.50	11.00	38.1	279.4	1	78.5	39.1	23.9	10.9	7.3	5.3	12.2	13.54 (87.35)	24	K, R	5395
1.50	11.00	38.1	279.4	1	391	180	118	57.1	38.9	27.3	60.6 13.6	14.77 (95.29)	24	K, R	5396
1.50	12.00	38.1	304.8	1	85.6	42.8	25.8	11.8	7.8	5.8	13.3	14.84 (95.74)	24	K, R	5397
1.53	3.05	38.9	77.5	8	176	88.4	53.4	25.7	17.6	12.3	27.3 6.2	3.89 (25.10)	26	K, R	5398
1.55	3.05	39.4	77.5	1	130	65.3	39.5	19.1	13.1	9.1	20.2	4.06 (26.19)	26	K, R	5399
1.61	2.15	40.9	54.6	1	205	102	54.5	27.3			31.8 7.2	3.00 (19.35)	30	K, R	5400
1.62	2.77	41.1	70.4	1	166	81.1	48.6	23.3	15.9	11.2	25.7 5.8	3.95 (25.48)	30	K, R	5401
1.65	3.00	41.9	76.2	2	128	64.1	38.8	18.3	12.8	8.9	19.8	4.50 (29.03)	30	K, R	5402
1.65	5.00	41.9	127.0	1	162	81.1	48.9	23.5	16.1	11.3	25.1 5.6	7.44 (48.00)	26	K, R	5403
1.70	5.10	43.2	129.5	1	580	290	154	77.2			89.9 20.4	7.77 (50.13)	24	K, R	5404
1.75	1.75	44.5	44.5	21	200	104	56.8	26.3	19.5	14.7	31.0 7.0	2.86 (18.45)	30	K, R	5592
1.75	2.73	44.5	69.3	2	159	79.5	48.1	23.1	15.8	11.1	24.6 5.6	3.77 (24.32)	26	K, R	5405
1.76	4.79	44.7	121.7	1	330	165	87.9	43.9	29.3	22.1	51.2 11.6	7.56 (48.77)	30	K, R	5406
1.78	4.30	45.2	109.2	1	737	369	196	98.1			114 26.1	6.66 (42.97)	30	K, R	5407

*Resistance tolerance is ±10% or ±0.5 , whichever is greater
 Rubber (HR) models not available with NiFe element

Standard
Polyimide
& Rubber





PRODUCT BULLETIN

Polyester Netting

Polyester or Dacron netting from Sheldahl is typically used as a spacer material to minimize conductive heat transfer between multilayer insulation (MLI) blanket layers. The netting material is chosen for its low outgassing characteristics and is specially cleaned to assure that it is residue free.

Sheldahl offers two types of netting; B2A and B4A. The B2A netting is a denser weave and is somewhat easier to handle. The B4A netting is used in applications where minimizing the blanket weight is critical. Both types of netting are supplied in rolls that are 54 inches wide.

PRODUCT CHARACTERISTICS

Parameter	Specified Value	
	B2A	B4A
Netting type	B2A	B4A
Weight (oz./sq. yd.)	≤0.44	≤0.21
Intermittent temperature range	-250° C to 150° C (-420° F to 300° F)	
Continuous temperature range	-250° C to 120° C (-420° F to 250° F)	
Thickness (in.)	0.007±0.001	0.0065±0.001
Burst strength (psi)	≥15	≥10
Construction (mesh/sq. in.)	190	43
Item number	147298	147096
Old part number	F022500	F020400

ALTERNATE LAYER SEPARATION TECHNIQUES

Using polyester netting is the most common way of separating the metallized film layers in MLI blankets. Two other options are available if polyester netting is not used.

Nomex

If the internal blanket temperature is too high for polyester, a Nomex scrim can be used. The Nomex netting or scrim is thicker than the polyester netting and weighs more than four times as much as B4A netting.

Embossing

Another approach to separating the blanket layers is to emboss the film. To achieve a small amount of separation between layers, a square tile pattern can be embossed into the film. The material is embossed to a depth of about 75 microns with a series of cross and down web lines every 3 mm (0.125 in.).

Our ShelTherm pattern embosses a series of dimples as deep as two to three millimeters. This pattern is more commonly used on PET films than on polyimide films.

SHELF LIFE

This product shall meet specified values for a minimum of 12 months after the date of shipment provided that the material is stored in its original unopened container at normal interior temperatures (10° C to 27° C/50° F to 80° F).

Sheldahl manufactures a broad range of vacuum deposited films, laminates and tapes. Ask for additional product bulletins describing other Sheldahl products.

The information on this product bulletin is based on data obtained by our research and is considered accurate. However, no warranty is expressed or implied regarding the accuracy of these data and the results obtained from the use thereof. This information is furnished upon the condition that the recipient shall conduct tests to determine the suitability of the product for his or her particular application.

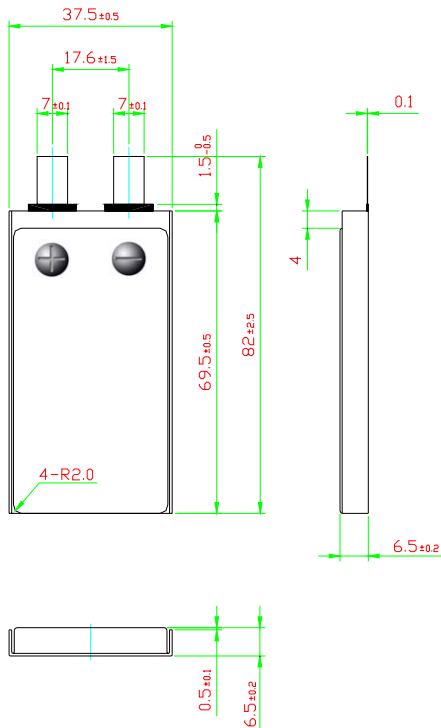
Cell Specification Data

SLB 603870H



Kokam Co., Ltd.

Cell Specification



● Typical Capacity ¹⁾		1.5 Ah
● Nominal Voltage		3.7 V
● Charge Condition	Max. Current	3.0 A
	Voltage	4.2V ± 0.03V
● Discharge Condition	Continuous Current	12.0 A
	Peak Current	24.0 A
	Cut-off Voltage	2.7 V
● Cycle Life		> 500 Cycles
● Operating Temp.	Charge	0 ~ 40 °C
	Discharge	-20 ~ 60 °C
● Dimension	Thickness (mm)	6.5 ± 0.2
	Width (mm)	37.5 ± 0.5
	Length (mm)	69.5 ± 0.5
● Weight (g)		32.0 ± 1.0

1) Typical Capacity : 0.5C, 4.2 ~ 2.7V @25°C,